An Efficient Zeolite-Supported Nickel-Iron Bimetallic Heterogeneous Catalyst for Hydrodeoxygenation of Vanillin: A Lignin Model Compound

Dissertation submitted to
Visvesvaraya National Institute of
Technology, Nagpur in fulfillment of the
requirement for the award of
the degree of

Master of Science in

Chemistry

By

RAKESH KUMAR TRIPATHY

(MS23CHM006)

under the guidance of

Dr. Jayant D. Ekhe

Professor

Department of Chemistry

Visvesvaraya National Institute of Technology

Nagpur 440 010 (India)

May 2025

An Efficient Zeolite-Supported Nickel-Iron Bimetallic Heterogeneous Catalyst for Hydrodeoxygenation of Vanillin: A Lignin Model Compound

Dissertation submitted to
Visvesvaraya National Institute of
Technology, Nagpur in fulfillment of the
requirement for the award of
the degree of

Master of Science in

Chemistry

By

RAKESH KUMAR TRIPATHY
(MS23CHM006)

under the guidance of

Dr. Jayant D. Ekhe

Professor

Department of Chemistry

Visvesvaraya National Institute of Technology

Nagpur 440 010 (India)

May 2025

© Visvesvaraya National Institute of Technology (VNIT) 2025

Department of Chemistry
Visvesvaraya National Institute of Technology Nagpur

Declaration

I, **Rakesh Kumar Tripathy**, hereby declare that this dissertation titled "(**An Efficient Zeolite-Supported Nickel-Iron Bimetallic Heterogenous Catalyst for Hydrodeoxygenation of Vanillin: A Lignin Model Compound)**" is carried out by me in the Department of Chemistry of Visvesvaraya National Institute of Technology, Nagpur. The work is original and has not been submittedearlier whole or in part for the award of any degree/diploma at this or any other Institution/ University.

Rakesh Kumar Tripathy
Name And Signature
Date:

Certificate

This to certify that the dissertation titled "(**An Efficient Zeolite-Supported Nickel-Iron Bimetallic Heterogenous Catalyst for Hydrodeoxygenation of Vanillin: A Lignin Model Compound)**" is submitted by **Rakesh Kumar Tripathy** in partial fulfillment of the requirements for the award of the degreeof **Master of Science in Chemistry**, VNIT Nagpur. The work is comprehensive, complete and fit for final evaluation.

Dr. Sujit Kumar Ghosh
Head of Department
Department of Chemistry
VNIT, Nagpur
Date:

Dr. Jayant D. Ekhe
Professor
Department of Chemistry
VNIT, Nagpur
Date:

Non-plagiarism certificate

It is certified that M.Sc. dissertation titled **"An Efficient Zeolite-Supported Nickel-Iron Bimetallic Heterogenous Catalyst for Hydrodeoxygenation of Vanillin: A Lignin Model Compound)"** by **Rakesh Kumar Tripathy** bearing Enrolment No. **MS23CHM006**, ID No. **30219** has been examined by us with the following anti-plagiarism tools.

The thesis has been checked using TURNITIN (copy of originally report attached) and found within limits as per HEC Plagiarism Policy and instructions issued from time to time.

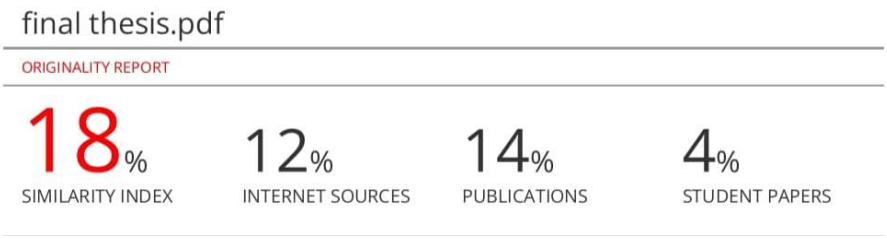

Dr. Jayant D. Ekhe
Professor
Department of Chemistry
VNIT, Nagpur
Date :

Rakesh Kumar Tripathy
(MS23CHM006)
Date:

Acknowledgement

I would like to express a deep sense of gratitude and sincere thanks to my project supervisor Dr. Jayant Ekhe, Professor of the Department of Chemistry, for his valuable guidance, encouragement, suggestions, and moral support throughout the period of my project work. It has been a privilege for me to work under his valuable guidance.

Gratitude is also accorded to VNIT, Nagpur for providing all the necessary facilities to complete the project work. My special thanks to Dr. Prem Lal Patel, Director of the Institute,for providing the necessary infrastructure and other facilities to pursue my project work successfully.

I express my special thanks to Dr. Sujit Kumar Ghosh, Professor, Head of the Department of Chemistry.

I am greatly thankful to Research scholars Mr. Kamleshwar Patle and Miss. Pooja Pardhi for valuable support & help throughout the research project, and also thankful to Mr. Swagat Pantawane, Miss. Vaishnavi Kolhtkar, & Miss. Mayuri Shende for helping in work and maintaining healthy, joyful environment in lab.

I would like to express my sincere thanks to the Department of Chemistry for facilitating the experimental and analytical instruments required for my project work and for permitting me to utilize their respective laboratory facilities to carry out my project work.

I express my special thanks to the Department of Chemistry, VNIT, Nagpur supportedby **DST FIST Project No. SR/FST/ CSI-279/2016(C)** for PXRD Data collection wherever this data will be reported.

My sincere thanks and appreciation are extended to the faculty members of the Departmentof Chemistry, Dr. Suresh S. Umare, Dr. Sujit K. Ghosh, Dr. Anupama Kumar, Dr. Ramani V. Motghare, Dr. Chayan Das, Dr. Atul V. Wankhade, Dr. Sangesh P. Zodape, Dr. Umesh R. Pratap, Dr. Susanta K. Nayak, Dr. Sorokhaibam Laxmi Gayatri, Dr. Abhishek Banerjee, Dr. Sandipan Halder.

Abstract

The selective hydrodeoxygenation (HDO) of lignin-derived oxygenated compounds into valuable aromatic hydrocarbons represents a critical step toward the sustainable valorization of renewable biomass resources. In this work, a cost-effective, non-noble metal-based bimetallic Ni2Fe@HZSM-5 catalyst was developed and systematically evaluated for its efficiency in converting lignin model compounds, particularly vanillin, under mild reaction conditions. The catalyst was synthesized by co-impregnation of iron and nickel precursors onto a HZSM-5 zeolite support, achieving a total metal loading of 10 wt.% with a Ni:Fe atomic ratio of approximately 2:1. The high surface area and strong Brønsted acidity & Lewis acidity of HZSM-5 provided an excellent platform for the fine dispersion of metal nanoparticles, essential for achieving superior catalytic activity. Extensive characterization using X-ray diffraction (XRD), scanning electron microscopy coupled with energy-dispersive X-ray spectroscopy (SEM-EDS), pyridine-adsorbed Fourier-transform infrared spectroscopy (Py-FTIR), Brunauer–Emmett–Teller (BET) surface area analysis, thermogravimetric analysis (TGA), and potentiometric acid strength measurements confirmed the uniform distribution of metal species, strong metal-support interactions, and excellent thermal stability of the prepared catalyst. Catalytic tests were conducted at 200°C Catalytic tests were performed using isopropanol (IPA) as both the reaction solvent and the in situ hydrogen donor, without the use of any external hydrogen gas. The Ni2Fe@HZSM-5 catalyst achieved complete conversion of vanillin with higher selectivity towards creosol formation with 80% yield, while guaiacol showed negligible conversion under identical conditions. The presence of the para-hydroxyl group in vanillin was found to facilitate selective reduction of the aldehyde group, aligning with literature reports that electron-donating groups enhance the reactivity of aromatic aldehydes. Iron played a vital role in improving nickel dispersion and modifying its electronic properties, thereby enhancing hydrogen activation. Concurrently, the acidic sites of HZSM-5 activated the carbonyl group of vanillin, enabling a strong synergy between the metal and acid sites. The proposed reaction mechanism involves initial adsorption of vanillin, hydrogenation to vanillyl alcohol, acid-catalysed dehydration to an intermediate, and subsequent hydrogenation to produce creosol. Isopropanol served not only as a hydrogen donor but also helped stabilize reaction intermediates and minimized coke formation, contributing to improved catalyst longevity.

List of Figures:

Figure 1.1 Catalytic Conversion of Lignin Model Compounds 2

Figure 1.2: Biomass-Derived Aromatics Conversion to Value-Added Products 4

Figure 1.3 Cellulose 5

Figure 1.4 Hemicellulose 5

Figure 1.5: Lignin Model Compounds 8

Figure 1.6: Block structure & composition of Cellulose, Hemicellulose & lignin in Biomass 9

Figure 1.7: Phenolic Monomer derived from lignin 10

Figure 1.8: Schematic Representation of Catalytic Reaction Mechanism and Mass Transfer Steps 12

Figure 1.9: Structure Of HZSM-5 17

Figure 1. 9:Basic structure of Zeolite 17

Figure 1.10: Structure of different zeolites **17**

Figure 2.1 Annual World energy supply 2007-17 ..... **20**

Figure 2.2 Vanillin synthesis by lignin **22**

Figure 3.1: An overview of the synthesis of HZSM-5 support 33

Figure 3.2: Schematic Representation of Synthesis of NixFey@H-ZSM-5 catalysts 33

Figure 3.3: XRD Instrument 35

Figure 3.4: SEM Instrument 36

Figure 3.5: BET Instrument 37

Figure 3.6: FTIR Instrument 38

Figure 3.7: Close-batch reactor (Parr Illinios) 39

Figure 3.8: GC-MS & GC-FID Instrument 40

Figure 3.9 Calibration curve of Creosol and vanillin 40

Figure 4.1: XRD pattern for a different molar proportion of Ni & Fe supported HZSM-5. 43

Figure 4.2: FTIR spectrum for a different molar proportion of Ni & Fe supported HZSM-5. 44

Figure 4.3: SEM images of HZSM-5 (a-d), SEM images of Ni2Fe@HZSM-5 (e-h), EDS Spectrum (i), Average Particle size (j), and Elemental mapping (k) of Ni2Fe@HZSM-5 46

Figure 4.4: BET plots of (a,b) N2 adsorption-desorption isotherms, (c,d) Surface area plots, and (e,f) BJH pore size distribution plots of HZSM-5 and Ni2-Fe@HZSM-5 48

Figure 4.5: Thermal properties of HZSM-5 & Ni2-Fe@HZSM-5 (a) TGA (b) DTG (c) DTA 49

Fig. 4.6 Optimization of reaction conditions for the conversion of vanillin to creosol 54

Figure 4.7: Catalytic Reaction Pathways 56

Figure 4.8: Plausible Catalytic Reaction Mechanism 56

Figure 4.10 GC-Chromatogram for optimized reaction condition 57

Figure 4.11: Mass spectrum of Creosol 58

Figure 4.12: Mass spectrum for ether…….. 58

List of Table:

Table 1.1: Elemental Composition Comparison of Wood-Based Bio-Oil and Fossil Fuel 7

Table 1.2: HZSM Characteristics **17**

Table 1.3: Hydrodeoxygenation Performance of Various Catalysts Under Batch Reactor Conditions 24

Table 1.4: Catalytic Performance for HDO of vanillin: Conversion, Selectivity, and Main products under various conditions 26

Table 1.5: Comparison of Catalysts for Hydrodeoxygenation (HDO) of Vanillin: Reaction Conditions, Conversion, Main Products, and Selectivity 29

Table 3.1: List of chemicals used in Catalyst synthesis & HDO reaction 31

Table 4.1 Physicochemical properties (BET surface area, pore volume, & pore radius) of HZSM-5 and Ni2Fe@HZSM-5 47

Table 4.2: Optimization of Fe–Ni Molar Proportion in Catalyst Composition 53

Table 4.3: Influence of Catalyst Dosage 53

Table 4.4: Effect of Reaction Temperature on Product Distribution 53

Table 4.4: Influence of Catalyst on Time 54

Nomenclature

Abbreviations

GC-MS-Gas chromatography-mass spectrometry

FTIR-Fourier transform infrared spectroscopy

HDO-Hydrodeoxygenation

H-ZSM-5-Zeolite Socony mobil-5

IPA-Isopropyl Alchol

BET-Braunauer Emmett Teller

SEM- Scanning electron microscope

EDS- Energy dispersive X-ray Spectroscopy

XRD-X-ray crystallography

p^H- Potential of hydrogen

MFI- Metamodel framework for interoperability

Symbols and subscripts

Psi-pound square per inch

rpm- revolution per Minute

Pm- picometre

pKa- Negative value of the logarithm of Ka

mv- millivolt

kPa- kilopascal is a unit of pressure

CONTENTS

Declaration

Certificate

Non-Plagiarism certificate

Acknowledgement

Abstarct

List of Figure

List of Table

Nomenclature

List of Publication

CHAPTER 1: INTRODUCTION 1

1. Introduction 2

1.1 Biomass valorization and its industrial relevance 3

1.1.1 Cellulose: 5

1.1.2 Hemicellulose: 5

1.1.3 Lignin: 5

1.2 Bio-oils and Representative Model Compounds 6

1.3 Properties of Bio-oils 6

1.4 Lignin and its potential Applications 8

1.4.1 Vanillin as a Lignin-Derived Model Compound 10

1.5 Role of Heterogeneous Catalysis in Biomass Conversion: 11

1.6 Hydrodeoxygenation (HDO) as a Key Upgrading Strategy: 12

1.6.1 Challenges in Vanillin Hydrodeoxygenation: 13

1.7 Zeolite-Supported Catalysts and Their Advantages: 15

1.7.1 Role and Structural Features of Zeolites: 16

CHAPTER 2: LITERATURE REVIEW 19

2.1 Biomass Valorization and Its Industrial Relevance: 21

2.2 Vanillin as a Model Compound for Lignin Conversion: 22

2.3 Progress in Hydrodeoxygenation Catalysis: 22

2.4 Application of Bimetallic Catalysts in Hydrodeoxygenation (HDO) 24

2.5 Zeolite-Supported Catalysts in Biomass Upgrading: 27

2.6 Solvent Effects in Hydrodeoxygenation Reactions: 28

CHAPTER 3: MATERIALS AND METHODS 30

3.1 Chemicals and Reagents: 33

3.2 Experimental: 31

3.2.1 Catalyst Preparation 32

3.2.1a Synthesis of HZSM-5: 33

3.2.2b Synthesis of Ni_xFe_y@HZSM-5 Catalysts: 34

3.3 Catalyst Characterization 34

3.3.1 Powder X-ray Diffraction (PXRD) Analysis 35

3.3.2 SEM 36

3.3.3 BET 37

3.3.4 FTIR 38

3.3.5 TG-DTA 38

3.4 Catalytic Reaction: 39

3.4a Sample Analysis: 39

3.4b Calibration Curve Analysis 40

3.5 Optimization Studies 40

CHAPTER 4: RESULTS AND DISCUSSION 42

4.1 Characterization of Catalysts: 54

4.1.1 PXRD Analysis 43

4.1.2 FTIR Analysis 44

4.1.3 SEM-EDS 45

4.1.4 N_2- Adsorption Desorption 47

4.1.5 Thermogravimetric Analysis (TGA) 49

4.2 Catalyst Screening and Optimization 50

4.2.1 Catalyst Composition Screening 50

4.2.2 Influence of Reaction Temperature 51

4.2.3 Influence of Catalyst Dosage 52

4.2.4 Influence of Reaction Time 53

4.2.5 Overall Assessment of Catalytic System 54

4.3 Proposed Reaction Pathway 55

4.3.1 Stepwise Plausible Reaction Mechanism 56

4.3.2 Role and Fate of Di(isopropyl) Ether Intermediate 57

4.3.3 Correlation with GC-MS Analysis 58

CHAPTER 5: CONCLUSION AND FUTURE SCOPE 60

5.1 Conclusion 61

5.2 Catalyst Characterisation 61

5.3 Catalytic Evaluation 61

5.4 Quantitative Analysis 61

5.5 Future Scope 62

5.5.1 Catalyst Development 62

5.5.2 Process Optimization 62

5.5.3 Feedstock Versatility 62

5.5.4 Sustainability and Integration 62

CHAPTER 1: INTRODUCTION

Introduction

The growing global concern over fossil fuel depletion and climate change has driven intense interest in renewable and sustainable energy sources. Among the various alternatives, lignocellulosic biomass stands out as a promising feedstock due to its abundance, renewability, and carbon-neutral nature[1]. It consists primarily of cellulose, hemicellulose, and lignin. While cellulose and hemicellulose are widely explored for bioethanol production, lignin remains underutilized despite being the most abundant renewable source of aromatic compounds[2].

Efficient valorization of lignin-derived compounds is essential for the economic viability of integrated biorefineries. Vanillin, one of the most accessible and well-defined model compounds derived from lignin, contains functional groups such as hydroxyl, methoxy, and aldehyde, making it a suitable probe molecule to study catalytic deoxygenation processes. The hydrodeoxygenation (HDO) of vanillin leads to the formation of valuable intermediates like guaiacol, creosol, and other alkylated phenols that can serve as fuel additives and chemical building blocks[3].

Catalytic upgrading of such oxygen-rich compounds requires efficient catalysts capable of selectively cleaving C–O bonds while preserving the aromatic structure. Heterogeneous catalysis provides a viable route due to advantages such as reusability, structural tunability, and process scalability. Transition metals like nickel (Ni) and iron (Fe) are widely used for their hydrogenation and hydrogenolysis capabilities. When used in bimetallic form, these metals often exhibit synergistic effects that enhance catalytic activity and stability[4].

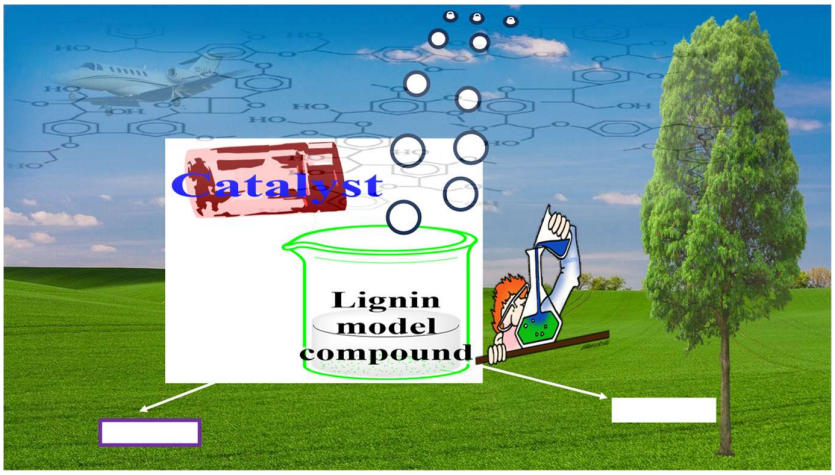

Figure 1.1: Catalytic Conversion of Lignin Model Compounds

The performance of these active metals is further influenced by the choice of support material. Zeolites, especially H-ZSM-5, are known for their high surface area, strong acidity, and shape-selective microporous structures. These properties enable selective access to the active sites and facilitate controlled reactions. When Ni and Fe nanoparticles are dispersed on H-ZSM-5, the resulting bifunctional catalyst combines the benefits of both metallic and acidic functionalities, making it highly effective for the HDO of vanillin[5].

1.1 Biomass valorization and its industrial relevance

The ongoing global transition toward sustainable development has intensified the demand for renewable resources to replace finite fossil-based materials. Environmental concerns, particularly those related to carbon emissions, climate change, and energy security, have driven the exploration of alternative feedstocks. Among the various renewable resources available, biomass stands out due to its abundance, carbon-neutral nature, and capacity to be transformed into a diverse range of fuels, chemicals, and materials[6].

Biomass refers to organic matter derived from plant and animal sources, including agricultural residues, forestry by-products, energy crops, and organic municipal waste. It primarily consists of three major components: cellulose, hemicellulose, and lignin. While cellulose and hemicellulose have traditionally been utilized for producing fermentable sugars and bioethanol, lignin remains significantly underutilized, often burned as a low-value energy source. However, the aromatic and chemically diverse structure of lignin presents considerable potential for the production of valuable chemical intermediates[7].

Valorization of biomass involves the conversion of these biological materials into high-value products through chemical, thermochemical, or biochemical processes. The aim is to derive not only energy carriers such as bioethanol, biodiesel, and syngas, but also platform chemicals that serve as building blocks for polymers, solvents, pharmaceuticals, and specialty chemicals[1]. Efficient utilization of biomass through valorization strategies is critical for the development of integrated biorefineries, which seek to replicate the functionality of petroleum refineries using renewable feedstocks[7].

From an industrial perspective, biomass valorization aligns with principles of green chemistry and circular economy. It promotes the reduction of greenhouse gas emissions, encourages the use of non-toxic and biodegradable materials, and supports energy

diversification. Furthermore, biomass-based industries contribute to regional development by utilizing locally available resources and generating rural employment[8].

In recent years, the development of selective and stable catalytic systems has become central to biomass conversion technologies. The use of heterogeneous catalysts, especially those based on earth-abundant metals, has shown promise for the selective upgrading of biomass-derived compounds under relatively mild conditions[4]. This thesis focuses on the hydrodeoxygenation (HDO) of vanillin, a lignin-derived model compound, using a zeolite-encapsulated Ni–Fe bimetallic catalyst, with the goal of developing an efficient and selective route for oxygen removal while preserving aromatic functionality[9].

Figure 1.2: Biomass-Derived Aromatics Conversion to Value-Added Products

Lignocellulosic biomass is a renewable and abundant resource primarily composed of three major biopolymers: cellulose, hemicellulose, and lignin. The efficient valorization of biomass into fuels and chemicals necessitates a fundamental understanding of these constituents, as their structural and chemical heterogeneity significantly influences biomass processing and conversion strategies[10].

1.1.1 Cellulose:

Cellulose is the most abundant organic polymer on the Earth, representing 35–50% of the dry weight of lignocellulosic biomass, depending on the plant species and cell type [9]. It is a linear polysaccharide composed of β-1,4-linked D-glucose units, with a degree of polymerization ranging from several hundred to over ten thousand[11]. The linear chains of cellulose align parallel to each other and are held together by extensive intra- and intermolecular hydrogen bonds, resulting in a highly ordered, crystalline structure.

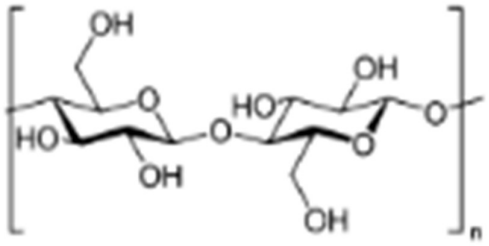

Figure 1.3 Cellulose

1.1.2 Hemicellulose:

Hemicellulose constitutes approximately 20–35% of the dry biomass and is markedly different from cellulose in both structure and composition [9]. It is a heterogeneous group of branched polysaccharides with a lower degree of polymerization (typically around 200). Hemicelluloses are composed of various monosaccharides, including pentoses (e.g., xylose, arabinose), hexoses (e.g., glucose, galactose, mannose), and uronic acids. Due to their branched and irregular structure, hemicelluloses are largely amorphous and more easily hydrolyzed than cellulose. Among the various types of hemicelluloses, xylan is the most abundant and consists of β-D-xylopyranosyl units linked primarily by β-1,4-glycosidic bonds[12].

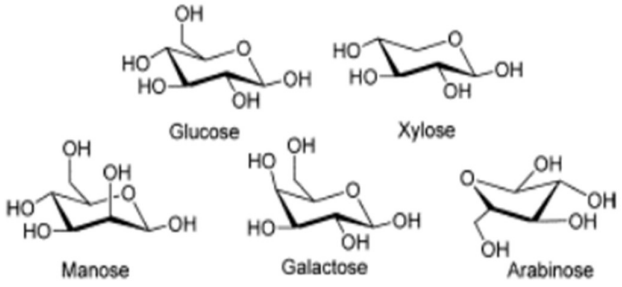

Figure 1.4 Hemicellulose

1.1.3 Lignin:

Lignin accounts for approximately 10–25% of the biomass dry weight and is a highly complex, amorphous, and cross-linked phenolic polymer [9–11]. Unlike cellulose and hemicellulose, lignin is not composed of repeating sugar units. Instead, it is synthesized

from three primary monolignols: coniferyl alcohol, p-coumaryl alcohol, and sinapyl alcohol. These monomers are linked through various types of ether and carbon-carbon bonds, including alkyl-aryl, aryl-aryl, and alkyl-alkyl linkages[12]. The resulting structure lacks uniformity and is highly variable depending on the plant species and tissue type[13]. Lignin functions as a binding agent, providing rigidity, hydrophobicity, and resistance to microbial attack by embedding cellulose and hemicellulose within the plant cell wall matrix[14].

1.2 Bio-oils and Representative Model Compounds

The conversion of lignocellulosic biomass into liquid fuels via thermochemical methods, particularly fast pyrolysis, represents a promising route for sustainable biofuel production. Fast pyrolysis involves the rapid thermal decomposition of biomass at moderate temperatures (typically 450–600 °C) under an inert atmosphere and very short vapor residence times (usually less than two seconds). This process efficiently breaks down the complex structure of biomass into a mixture of products, with bio-oil being the primary output[15].

Bio-oils derived from fast pyrolysis can account for up to 75% of the total product yield, depending on the feedstock and operating conditions [2,12,13]. These bio-oils are complex mixtures containing a wide range of oxygenated organic compounds, including aldehydes, ketones, alcohols, carboxylic acids, furans, and phenolic derivatives. The high oxygen content of these compounds, while characteristic of biomass-derived oils, poses challenges such as acidity, instability, and low heating value, necessitating further upgrading[16].

The lignin-derived fraction of bio-oil is particularly rich in aromatic compounds due to the phenolic nature of lignin. Key aromatic products include phenol, anisole, guaiacol (which can constitute nearly 39% of lignin pyrolysis liquids), along with cresols, syringol, and their methylated derivatives. These phenolic compounds are valuable both as fuel precursors and as platform chemicals for fine chemical synthesis.[17]

1.3 Properties of Bio-oils

The properties of bio-oil derived from fast pyrolysis are influenced by the feedstock used and the specific operating conditions. One of the most notable characteristics of bio-oil is its high oxygen content, which can account for up to 40 wt.% of its composition. The presence of oxygen significantly impacts the properties of the bio-oil, making it less stable

and limiting its direct application as a fuel in conventional petroleum infrastructure. Additionally, bio-oil contains a substantial amount of water (up to 30 wt.%), further complicating its utilization [18].

From a chemical standpoint, bio-oil is acidic, with a pH ranging from 2.8 to 3.8, a feature that arises from its high concentration of carboxylic acids and other oxygenated compounds. Its viscosity is relatively high, and it has a low heating value, often less than half of that of petroleum fuels, primarily due to the oxygen content. This lower energy density can be attributed to the presence of large amounts of oxygenated functional groups such as aldehydes, ketones, phenolics, and acids. These groups contribute to the bio-oil's tendency to polymerize, leading to thermal and chemical instability over time. Additionally, bio-oil is immiscible with conventional petroleum, making it unsuitable for direct use in current infrastructure, which is designed to handle fossil-based fuels[17]

Given these challenges, bio-oil must undergo upgrading to enhance its fuel properties. One critical method to improve bio-oil quality is catalytic deoxygenation, which selectively removes oxygen to increase the energy density, stability, and compatibility of the bio-oil with conventional fuels. This process can significantly enhance the bio-oil's properties, making it more suitable for use as a high-quality transportation fuel or chemical feedstock.[19]

The table below presents a comparison of the elemental composition and physical properties of wood-based bio-oil and conventional fossil fuels, highlighting the substantial differences that must be addressed in upgrading bio-oils to make them viable for broader applications.[17]

Table 1.1: Elemental Composition Comparison of Wood-Based Bio-Oil and Fossil Fuel

Composition		
Elemental analysis	Wood-based bio-oil (wt.%)	Fossil fuel (wt.%)
carbon	40–50	85
hydrogen	6.0–7.6	11–13
oxygen	36–52	0.1–1.0
nitrogen	0.00–0.15	0.1
sulfur	0.00–0.02	1.0–1.8
water	17–30	0.02–0.1
solid	0.03–0.7	1

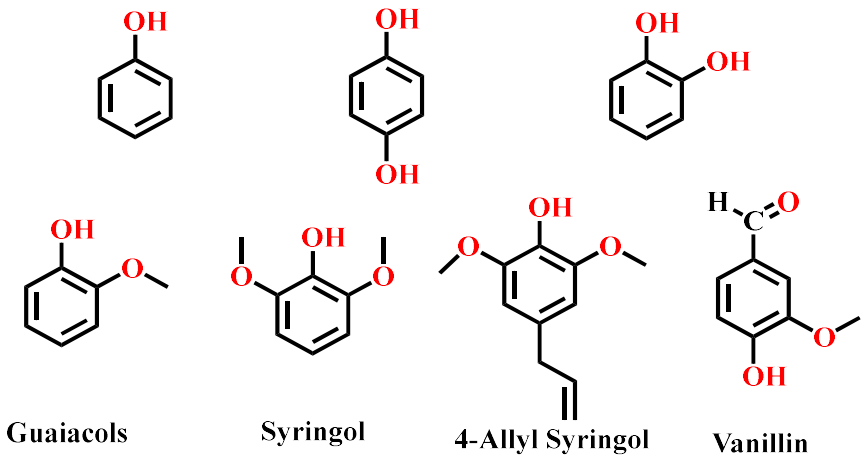

Figure 1.5: Lignin Model Compounds

1.4 Lignin and its potential

Lignin is one of the three primary constituents of lignocellulosic biomass, alongside cellulose and hemicellulose. Unlike its polysaccharide counterparts, lignin is a complex, irregular, and highly cross-linked aromatic polymer composed mainly of phenylpropanoid units. It accounts for approximately 15–30% of the dry weight of terrestrial plants and represents the largest natural reservoir of renewable aromatic carbon on Earth. Despite its abundance and structural richness, lignin has historically been considered a by-product of the pulp and paper industry, with most of it being incinerated for heat and energy.[20]

The structural complexity of lignin arises from the random polymerization of three primary monolignols: coniferyl alcohol, sinapyl alcohol, and p-coumaryl alcohol, which lead to the formation of guaiacyl (G), syringyl (S), and p-hydroxyphenyl (H) units, respectively. This heterogeneous and resistant architecture provides mechanical strength to plant cell walls but also poses challenges for its depolymerization and subsequent utilization. Nevertheless, the rich aromatic nature of lignin offers a unique opportunity to replace fossil-derived aromatic compounds in the production of bio-based chemicals and materials.[21]

Recent advancements in lignin depolymerization techniques—such as catalytic hydrogenolysis, oxidative cleavage, and solvolysis—have made it increasingly feasible to obtain low-molecular-weight aromatic compounds from lignin. Among these, vanillin, guaiacol, syringol, and ferulic acid have emerged as key platform molecules with

commercial potential. In particular, vanillin has garnered attention not only for its use as a flavoring agent but also as a model compound representing the chemical functionality and reactivity of lignin-derived aromatics[22].

Utilizing lignin as a feedstock aligns well with the goals of green chemistry and sustainable process development. By transforming this traditionally undervalued biomass component into high-value products, the economic viability and environmental performance of biorefineries can be significantly enhanced. Moreover, the valorization of lignin contributes to a more holistic and integrated approach to biomass conversion, where all major fractions are utilized effectively rather than discarded or combusted.

The present study focuses on the catalytic upgrading of vanillin, a compound derived from the oxidative cleavage of lignin. Vanillin's aldehyde, methoxy, and hydroxyl functionalities make it an ideal candidate for studying catalytic hydrodeoxygenation (HDO) reactions, which aim to remove oxygen while preserving the aromatic core. Effective transformation of vanillin into partially or fully deoxygenated compounds such as creosol can serve as a model for the broader valorization of lignin-derived molecules into fuels and specialty chemicals.[23]

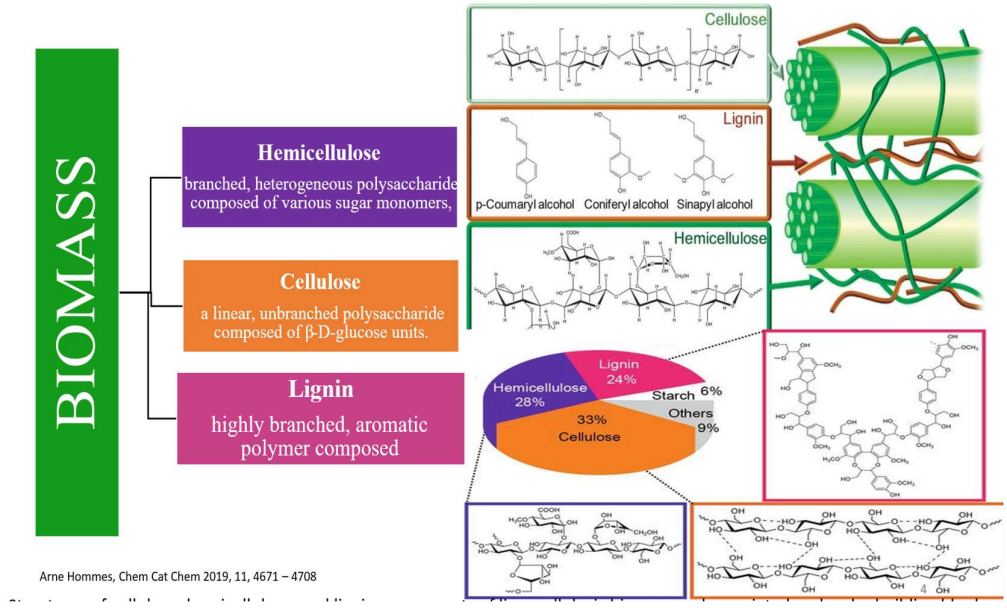

Figure 1.6: Blocks structure & composition of Cellulose, Hemicellulose & lignin in Biomass

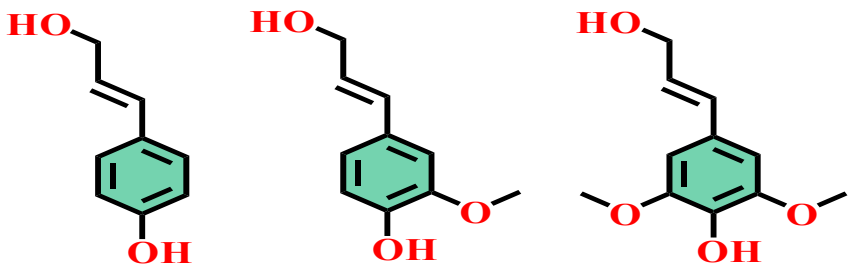

Figure 1.7: Phenolic Monomer derived from lignin

1.4.1 Vanillin as a Lignin-Derived Model Compound

Vanillin (4-hydroxy-3-methoxybenzaldehyde) is one of the most important aromatic compounds obtained from the depolymerization of lignin. Structurally, it contains a methoxy group (-OCH_3), a hydroxyl group (-OH), and an aldehyde functional group (-CHO) attached to an aromatic ring, making it a versatile platform molecule for catalytic studies. Naturally occurring in vanilla beans, vanillin is also produced industrially from lignin-derived feedstocks, particularly from spent sulfite liquor in the pulp and paper industry[24].

Due to its relatively simple structure and presence of both oxygenated and aromatic functionalities, vanillin is widely used as a model compound to study the transformation of lignin-derived molecules into valuable chemicals. It reflects many of the challenges encountered during lignin valorization, such as selective cleavage of C–O bonds, preservation of aromaticity, and management of multifunctional groups during catalytic upgrading.

The chemical reactivity of vanillin makes it an excellent candidate for exploring various catalytic transformations, including hydrogenation, hydrodeoxygenation (HDO), decarbonylation, and aromatic ring hydrogenation. In particular, the aldehyde group in vanillin is highly reactive under hydrogenation conditions, while the methoxy and hydroxyl groups pose challenges for selective deoxygenation. These functional groups simulate the behavior of more complex lignin-derived compounds, allowing researchers to test catalyst performance, reaction mechanisms, and selectivity trends under controlled conditions.[25]

In addition to its role in model studies, vanillin itself is a valuable compound with broad applications in the food, fragrance, and pharmaceutical industries. Its global demand has

driven interest in developing greener, more sustainable production routes from lignin rather than relying solely on petrochemical processes or natural extraction, which are limited by low yields and high costs.[25]

From a catalytic research perspective, vanillin offers several advantages. Its chemical behavior is well-documented, enabling meaningful comparisons across different catalytic systems and conditions. Moreover, its commercial availability and stability under various reaction environments make it suitable for both batch and continuous-flow studies.

In this thesis, vanillin is selected as the primary probe molecule to investigate the hydrodeoxygenation (HDO) performance of a zeolite-encapsulated Ni–Fe bimetallic catalyst. This approach aims to deepen understanding of selective C–O bond removal in aromatic oxygenates and to explore efficient routes for upgrading lignin-derived compounds into fuel-like or value-added aromatic products[26].

1.5 Role of Heterogeneous Catalysis in Biomass Conversion:

Heterogeneous catalysis plays a vital role in enabling efficient and selective biomass conversion processes. Unlike homogeneous catalysts, which are dissolved in the same phase as the reactants, heterogeneous catalysts exist in a separate solid phase and offer several practical advantages, including easy separation, regeneration, and reuse. These features are particularly valuable for large-scale biomass processing, where economic and environmental considerations are critical.

In the context of biomass conversion, heterogeneous catalysts contribute significantly to:

1. Selective deoxygenation of oxygenated bio-oil compounds,
2. Activation of hydrogen for reductive transformations,
3. Stabilization of reaction intermediates through support interactions,
4. Enhancement of product selectivity via acidic or metal-active sites.

Catalysts based on transition metals, especially Ni, Fe, Co, and Mo, supported on acidic materials like zeolites, alumina, or carbon, have shown notable performance in hydrodeoxygenation and hydrogenolysis reactions. The combination of metal sites for hydrogenation and acid sites for dehydration creates a bifunctional environment that is well-suited for breaking down complex bio-oil structures.[27]

Furthermore, zeolite-supported bimetallic catalysts, such as Ni-Fe on H-ZSM-5, offer tunable acidity, shape-selective pores, and enhanced metal dispersion. These features improve both the activity and stability of the catalyst while also minimizing undesirable side reactions such as over-hydrogenation or coking.[28]

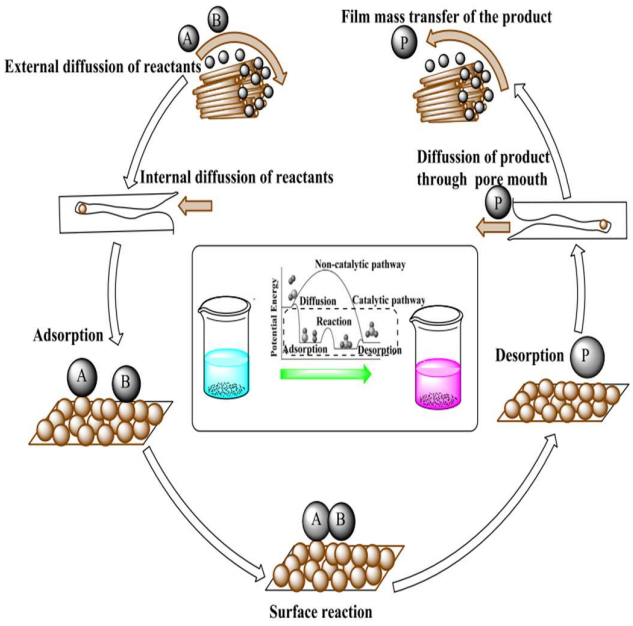

Figure 1.8: Schematic Representation of Catalytic Reaction Mechanism and Mass Transfer Steps

1.6 Hydrodeoxygenation (HDO) as a Key Upgrading Strategy:

Hydrodeoxygenation (HDO) is a vital chemical transformation in the upgrading of biomass-derived compounds, particularly those originating from lignin. These oxygen-rich molecules typically contain functional groups such as hydroxyl, methoxy, carbonyl, and carboxyl, which contribute to their high polarity, chemical instability, and low energy density. To convert such compounds into fuel-like or chemically valuable intermediates, selective removal of oxygen is essential. HDO facilitates this process by cleaving C–O bonds through the addition of hydrogen, usually in the presence of a metal-based catalyst under elevated temperature and hydrogen pressure.[28,29]

The primary goal of HDO is to reduce the oxygen content of bio-derived molecules without excessive loss of carbon or aromaticity. For compounds like vanillin, this involves transformation of the aldehyde group to a methyl group or alcohol, removal of methoxy or

hydroxyl groups, and retention of the aromatic ring when possible. These transformations yield products with improved stability, lower viscosity, and higher compatibility with petroleum-derived fuels or intermediates.[30]

Conventional HDO processes have been extensively applied in the petroleum refining industry, particularly in the hydroprocessing of heavy oils and phenolic compounds. However, the oxygenated and multifunctional nature of lignin-derived molecules introduces additional challenges. These include competing reaction pathways (e.g., hydrogenation vs. deoxygenation), the potential for catalyst poisoning by reactive oxygen species, and control over product selectivity.[31]

Typically, transition metal catalysts such as nickel (Ni), cobalt (Co), molybdenum (Mo), and noble metals like palladium (Pd) and ruthenium (Ru) are employed in HDO. These metals, when supported on acidic or porous carriers, facilitate hydrogen activation and promote C–O bond scission. The effectiveness of HDO strongly depends on several factors, including the nature of the metal, the support material, the type of solvent, and the reaction environment (temperature, hydrogen pressure, and time).

In recent years, efforts have shifted toward developing non-noble metal catalysts such as Ni and Fe due to their lower cost and favorable activity. Additionally, combining metals into bimetallic systems can enhance catalytic performance through synergistic effects, such as improved hydrogen activation or more efficient C–O bond cleavage.

HDO is not only important for producing stable and energy-dense fuel components but also plays a central role in synthesizing value-added chemicals from lignin-derived molecules. Its integration into biorefinery schemes is critical for ensuring the complete utilization of lignocellulosic biomass. The current research explores the HDO of vanillin using a Ni–Fe bimetallic catalyst encapsulated in zeolite, aiming to achieve selective deoxygenation under relatively mild and environmentally benign conditions.[32]

1.6.1 Challenges in Vanillin Hydrodeoxygenation:

Despite the promising potential of hydrodeoxygenation (HDO) for upgrading lignin-derived compounds, several technical and chemical challenges remain, especially when targeting molecules like vanillin. Vanillin’s multifunctional nature—comprising an aldehyde group, a hydroxyl group, and a methoxy substituent presents unique obstacles in

achieving selective and efficient deoxygenation without over-hydrogenation or undesirable side reactions.

One major challenge lies in the selectivity of C–O bond cleavage. Vanillin contains both phenolic and methoxy functionalities, which differ in bond strength and reactivity. The selective removal of these groups without compromising the aromatic ring or leading to full hydrogenation is often difficult. Competing reactions such as ring saturation, decarbonylation, or formation of polymeric by-products can reduce yield and selectivity toward the desired partially deoxygenated products, such as guaiacol or creosol.

Another issue involves the reactivity of the aldehyde group, which is highly susceptible to hydrogenation under HDO conditions. While this transformation can be favorable for producing more stable methylated products, uncontrolled hydrogenation can result in excessive reduction or loss of the oxygenated aromatic framework. Maintaining control over intermediate steps such as aldehyde-to-alcohol conversion or aldehyde-to-methyl reduction, is critical for guiding the reaction pathway toward target products.

The design and stability of the catalyst also pose significant challenges. Traditional HDO catalysts, especially those containing noble metals, may exhibit high activity but suffer from high costs and low tolerance to oxygenated compounds, which can lead to deactivation or leaching. In contrast, earth-abundant metals like Ni and Fe offer a more sustainable alternative but may require precise tuning to enhance their activity and resistance to deactivation. The tendency of active metals to agglomerate under thermal conditions can further reduce catalytic performance over time.

Additionally, reaction conditions, including temperature, hydrogen pressure, and solvent choice, strongly influence the reaction mechanism and product distribution. Elevated temperatures may enhance deoxygenation but also promote unwanted side reactions or catalyst sintering. Hydrogen pressure must be sufficient to drive C–O bond scission but should be optimized to prevent over-hydrogenation. The solvent plays a dual role, acting as a medium and sometimes participating in the reaction, affecting the solubility of vanillin and stabilization of intermediates.[33]

Finally, understanding the reaction mechanism and intermediate species remains an area of active research. Detailed knowledge of the reaction pathway is essential for improving

catalyst design and process control. However, the complexity of vanillin's structure and the variety of possible products make mechanistic studies challenging.

To address these issues, the present study employs a zeolite-encapsulated bimetallic Ni–Fe catalyst, aiming to enhance catalytic selectivity, metal dispersion, and stability. The use of a tailored support structure like zeolite can help regulate the local environment around active sites, reduce metal sintering, and potentially improve product distribution through shape-selective catalysis.[34]

1. Zeolite-Supported Catalysts and Their Advantages:

Zeolites are crystalline aluminosilicate materials characterized by their well-defined microporous structures, high surface area, thermal stability, and tunable acidity. These properties make them highly valuable as catalyst supports in various chemical transformations, including biomass conversion and hydrodeoxygenation (HDO) of oxygen-rich aromatic compounds. The combination of their structural regularity and chemical versatility enables zeolites to serve not only as passive supports but also as active participants in catalytic processes.

One of the key advantages of zeolites lies in their shape selectivity, which arises from their uniform pore networks. This allows zeolites to selectively admit or exclude reactant and product molecules based on size and shape, thereby influencing reaction pathways and enhancing product specificity. For lignin-derived molecules such as vanillin, this characteristic can help guide the reaction toward desired partially deoxygenated products while suppressing side reactions like condensation or ring hydrogenation.

The acidity of zeolites, originating from their framework aluminum sites, plays a critical role in activating oxygen-containing functional groups and facilitating C–O bond cleavage. The presence of Brønsted and Lewis acid sites can enhance the interaction between reactant molecules and the catalyst surface, promoting protonation or polarization of functional groups for subsequent reaction steps. When used in conjunction with metal catalysts, such as Ni and Fe, zeolite supports can promote bifunctional catalysis, where both metal and acid sites contribute synergistically to the overall reaction mechanism.

Zeolite supports also provide a high degree of thermal and mechanical stability, which is essential for reactions conducted at elevated temperatures and pressures, such as those typical of HDO processes. Their resistance to sintering and structural degradation ensures longer catalyst lifetimes and consistent performance over multiple reaction cycles.[35]

Encapsulation of metal nanoparticles within zeolite frameworks offers further benefits. The confined environment provided by the micropores can limit metal nanoparticle growth, thereby enhancing dispersion and preserving high surface area. This encapsulation can also prevent leaching and aggregation of metal particles during reaction, improving catalyst durability and recyclability. Moreover, the proximity of metal and acid sites within the zeolite matrix allows for enhanced cooperative catalysis, where sequential or tandem reactions occur more efficiently.

In this study, a Ni–Fe bimetallic catalyst encapsulated within a zeolite structure is utilized for the selective hydrodeoxygenation of vanillin. The use of zeolite as a support is expected to improve the dispersion of active metal species, stabilize the catalyst under reaction conditions, and influence product selectivity through shape-selective effects and acidic site interactions. This design aims to develop a cost-effective, recyclable, and efficient catalytic system for the valorization of lignin-derived aromatics[35]

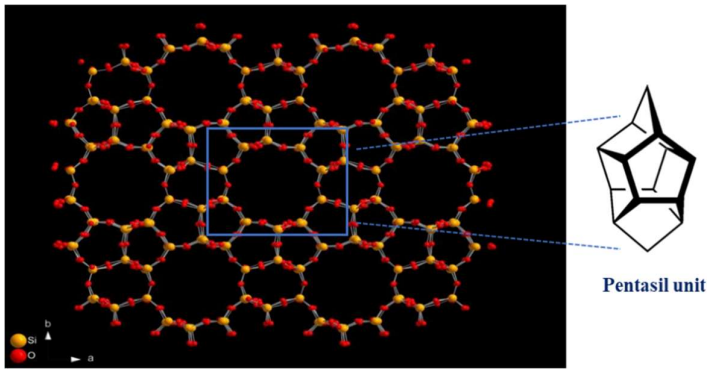

Figure 12: Structure Of HZSM-5

1.7.1 Role and Structural Features of Zeolites:

Zeolites are microporous, crystalline aluminosilicates that serve as highly effective catalysts and catalyst supports in various industrial processes, particularly in hydrocarbon conversion and biomass upgrading. Their catalytic efficiency arises from a unique

combination of strong Brønsted acidity, shape-selective microporous frameworks, and high thermal stability.[36]

The fundamental structure of a zeolite consists of interconnected SiO_4 and AlO_4 tetrahedra. These tetrahedra share oxygen atoms at the corners, creating a negatively charged three-dimensional framework. To balance this negative charge, the voids within the zeolite structure are typically occupied by exchangeable cations (e.g., Na^+, H^+) and water molecules. The porous network includes cages and channels ranging from 0.2 to 1 nm in size, which facilitate shape-selective catalysis—a phenomenon where the pore structure governs the accessibility and orientation of reactant molecules.

Zeolites are extensively used in the petrochemical and refining industries, and they have recently gained attention in biomass conversion applications, especially for processes like bio-alcohol dehydration and hydrodeoxygenation (HDO). Their framework structure allows selective passage and transformation of reactant molecules, making them ideal for catalytic upgrading of lignin-derived compounds.

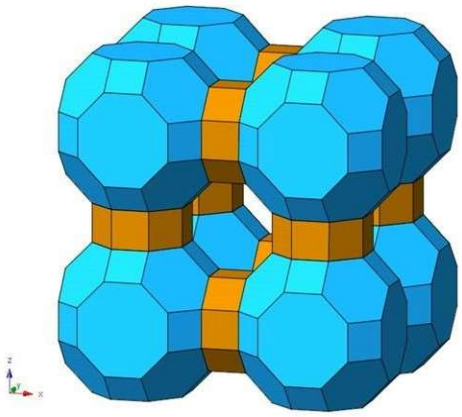

Figure 1. 9:Basic structure of Zeolite

Table 1.2: HZSM Characteristics

Material	Porosity	Acid type	Acid strength	crystallinity
HZSM-5	microporous	mostly Bronsted	strong	high

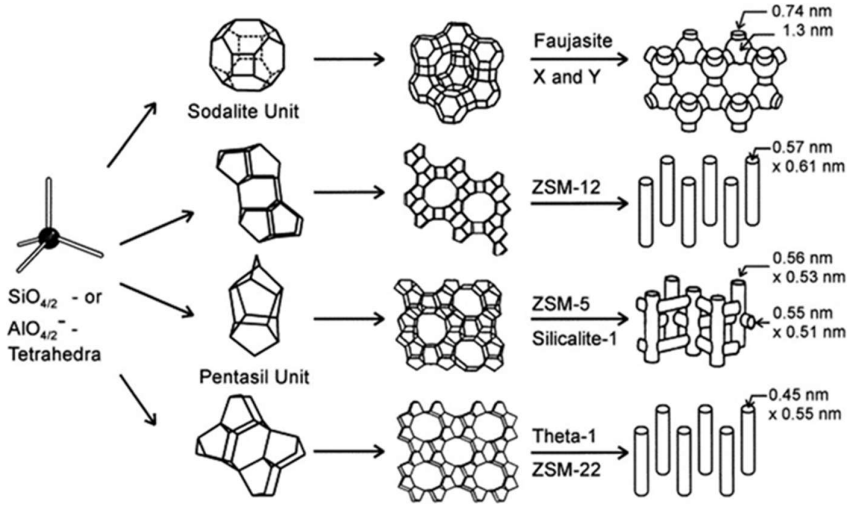

Figure 1.10: Structure of different zeolites

CHAPTER 2: LITERATURE REVIEW

2.1 Biomass Valorization and Its Industrial Relevance:

The growing demand for sustainable energy and chemicals has driven global research interest toward renewable feedstocks, among which biomass holds a prominent position. Biomass is an abundant and carbon-neutral resource that includes plant-derived materials such as lignocellulose, agricultural residues, and forestry waste. Unlike fossil fuels, biomass is continuously renewable and can be processed into a wide array of value-added products, including biofuels, bioplastics, and fine chemicals.

Within the biorefinery framework, lignocellulosic biomass is particularly attractive due to its widespread availability and potential for complete utilization. It is composed mainly of cellulose, hemicellulose, and lignin, each offering different chemical building blocks. While cellulose and hemicellulose are traditionally converted into sugars and then into bioethanol or platform chemicals, lignin, which accounts for approximately 15–30% of the biomass, remains largely underutilized despite being the richest natural source of aromatic compounds.

Industrial valorization of biomass, particularly through thermochemical and catalytic routes, is gaining momentum. Technologies such as pyrolysis, gasification, and hydrothermal liquefaction convert biomass into intermediates like bio-oil or syngas, which require further upgrading. Among various catalytic strategies, hydrodeoxygenation (HDO) has emerged as a key step in improving the stability, energy density, and compatibility of biomass-derived intermediates with petroleum-based systems. Efficient conversion of oxygenated bio-oils into hydrocarbons not only facilitates their integration into fuel infrastructures but also supports the global transition toward a circular and low-carbon economy[37].

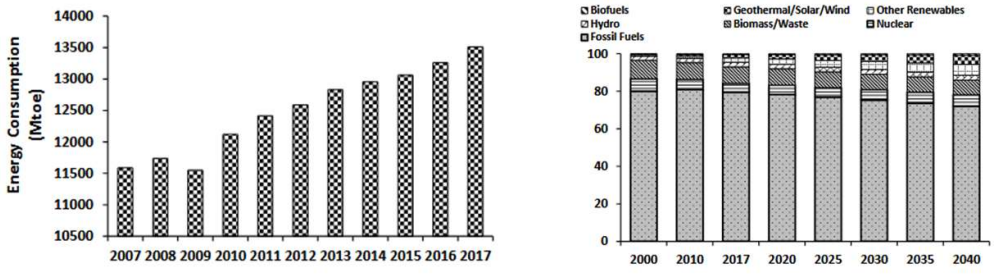

Figure 2.1 Annual World energy supply 2007-17

2.2 Vanillin as a Model Compound for Lignin Conversion:

Vanillin (4-hydroxy-3-methoxybenzaldehyde) is one of the most prominent and extensively studied monomeric compounds derived from the oxidative or reductive depolymerization of lignin. Due to its well-defined molecular structure, which includes an aldehyde group (-CHO), a hydroxyl group (-OH), and a methoxy group ($-OCH_3$) attached to an aromatic ring, vanillin serves as an ideal model compound to investigate the fundamental catalytic pathways in lignin valorization, especially via hydrodeoxygenation (HDO) processes.

Vanillin is industrially significant not only as a flavouring agent and fragrance but also as a platform molecule in bio-based chemical production. Its structure mirrors the complexity and diversity of lignin-derived molecules, representing the functional groups commonly found in lignin monomers. This makes it a suitable candidate for examining structure–reactivity relationships, particularly in the selective removal of oxygenated functionalities without compromising the aromatic integrity of the molecule[38].

In the context of hydrodeoxygenation, the reactivity of vanillin presents a set of challenges and opportunities. The aldehyde group is highly reactive and prone to hydrogenation to form vanillyl alcohol or further reduction to methylated derivatives such as 2-methoxy-4-methylphenol (creosol). The hydroxyl group, typically at the para-position, can be selectively removed via acid- or metal-catalyzed pathways. The methoxy group is more resistant to cleavage but can undergo demethylation under suitable catalytic conditions. Thus, the HDO of vanillin often proceeds through sequential or parallel reaction pathways, depending on the catalyst composition and reaction parameters[39].

The study of vanillin conversion is critical for evaluating catalyst performance in terms of activity, selectivity, and stability. Transition metal catalysts such as Ni, Co, Cu, Pd, and Fe have been investigated for this purpose, either in monometallic or bimetallic configurations. Nickel-based systems, in particular, exhibit high hydrogenation activity, while the addition of secondary metals like Fe can enhance the selectivity and tune the electronic properties of active sites. The interaction between the catalyst and the functional groups in vanillin determines the pathway followed—whether it favours full

deoxygenation, partial hydrogenation, or undesirable side reactions such as condensation or ring saturation.

Furthermore, vanillin serves as a diagnostic probe to understand reaction mechanisms and intermediate species formation during lignin upgrading. Using vanillin as a model allows for controlled experimental conditions and reproducible results, which are often difficult to achieve with complex lignin mixtures. Insights gained from vanillin HDO studies can be extrapolated to more complex systems, guiding the design of robust catalytic processes for broader lignin-derived compound upgrading.

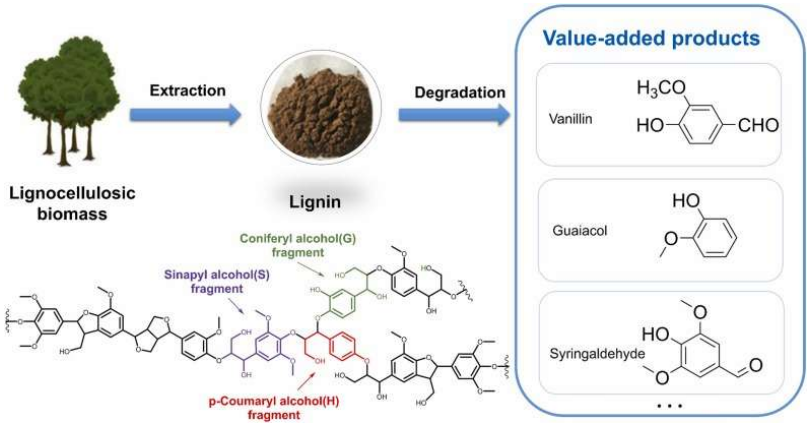

Figure 2.2 Vanillin synthesis by lignin

2.3 Progress in Hydrodeoxygenation Catalysis:

Hydrodeoxygenation (HDO) is a crucial catalytic process employed to upgrade oxygen-rich compounds derived from lignin and other biomass components into more stable and energy-dense hydrocarbon products. This transformation involves the selective removal of oxygen-containing functional groups such as hydroxyl, carbonyl, carboxyl, and methoxy groups through hydrogenolysis and hydrogenation reactions, often under elevated temperatures and pressures in the presence of hydrogen gas and metal catalysts. The successful application of HDO is central to enhancing the fuel quality and chemical compatibility of bio-oils with conventional petroleum-based systems.

Over the past two decades, significant progress has been made in the development of catalytic systems for HDO, focusing on improving conversion efficiency, product selectivity, and catalyst stability. Broadly, HDO catalysts can be classified into two categories: noble metal catalysts and non-noble (base) metal catalysts.

Noble metal catalysts such as Pt, Pd, Ru, and Rh have shown excellent activity and selectivity for the HDO of lignin-derived compounds. These metals possess high hydrogenation capability and can operate at relatively mild conditions. For instance, Pd-based catalysts have demonstrated effective deoxygenation of vanillin and guaiacol with minimal aromatic ring saturation. However, the high cost, limited availability, and susceptibility to poisoning by sulfur or nitrogen compounds present in biomass feedstocks limit the large-scale application of noble metals[40].

To overcome these limitations, attention has shifted toward base metal catalysts such as Ni, Co, Fe, and Cu. Among them, nickel-based catalysts have emerged as cost-effective alternatives with strong hydrogenation activity. Nevertheless, monometallic Ni catalysts often exhibit poor selectivity, especially in retaining aromaticity, and can suffer from deactivation due to sintering or coke deposition during prolonged operation. To address these issues, bimetallic systems, combining Ni with Fe, Co, or Cu, have been developed to enhance the performance and tailor the electronic and geometric structure of the active sites[41].

The reaction pathway of HDO is influenced by the nature of the substrate and the catalyst. For example, vanillin may undergo sequential hydrogenation of the aldehyde group to vanillyl alcohol, followed by deoxygenation to creosol and further demethylation or decarbonylation depending on the catalyst and reaction conditions. Therefore, controlling reaction selectivity is a major objective in catalyst design, aiming to suppress over-hydrogenation and avoid loss of valuable aromatic structure.

Recent studies have emphasized the importance of acid–metal bifunctional catalysts, where acidic supports (e.g., zeolites, alumina, or niobia) facilitate C–O bond cleavage, while metal sites activate hydrogen for reduction. Such systems promote tandem reactions, enabling efficient transformation of lignin monomers into hydrocarbons. The synergistic effect between metal and acid sites can greatly influence product distribution and minimize the formation of char or heavy oligomers.

Moreover, innovations in catalyst support materials, such as mesoporous silicas, carbon-based supports, and zeolites, have played a key role in improving metal dispersion, accessibility of active sites, and catalyst lifetime. Encapsulation techniques, particularly in

microporous zeolites, have demonstrated improved resistance to metal sintering and leaching, while providing shape-selective access to reactants.

Table 1.3: Hydrodeoxygenation Performance of Various Catalysts Under Batch Reactor Conditions

Catalyst	Reactor type	Yield of oil (wt%)	Deoxygenation (Wt%)	Temperature in (K)	Pressure (MPa)	Time (h)
$NiMoS/Al_2O_3$	Batch	30	36	523	10	4
Pd/C	Batch	43	56	523	10	4
Ru/C	Batch	35	41	523	10	4
$NiMoS/Al_2O_3$	Batch	27	74	523	10	4
Pd/C	Batch	65	85	623	10	4
$CoMoS/Al_2O_3$	Batch	25	82	623	10	4
Ru/C	Batch	53	86	623	10	4
$NiCu/TiO_2$	Batch	45.5	62	423	19	4
NiCu/Sibunite	Batch	35.9	86.5	423	19	4
$NiCu/Al_2O_3$	Batch	42.2	57.4	423	19	4

2.4 Application of Bimetallic Catalysts in Hydrodeoxygenation (HDO)

The applications of bimetallic catalysts in hydrodeoxygenation (HDO) processes have emerged as a promising strategy to overcome the limitations associated with monometallic systems. Bimetallic catalysts, which combine two different metallic components at the nanoscale, offer a unique set of advantages, including enhanced catalytic activity, improved selectivity, increased resistance to deactivation, and tunable electronic and geometric properties. These synergistic effects are particularly valuable in complex reactions such as the HDO of lignin-derived oxygenated aromatics, where multiple

reaction steps—such as hydrogenation, hydrogenolysis, and decarbonylation—occur simultaneously or sequentially[42].

In the context of lignin valorization, several bimetallic combinations have been explored, including Ni-Fe, Ni-Co, Ni-Cu, Co-Mo, and Pd-Fe systems. Among them, nickel-based bimetallic catalysts have attracted significant attention due to the abundance and cost-effectiveness of Ni and its well-known hydrogenation capability. The addition of a second metal, such as iron (Fe), can significantly alter the electronic density around the active Ni centers, modulating adsorption behavior and enhancing selectivity toward desired products[43].

For instance, Ni–Fe bimetallic catalysts supported on acidic or mesoporous supports have demonstrated notable performance in the HDO of vanillin and related compounds. The presence of Fe introduces redox properties and facilitates the cleavage of C–O bonds, particularly in methoxy and hydroxyl groups. Meanwhile, Ni primarily promotes hydrogenation of the carbonyl group. This division of function allows for more selective conversion pathways and reduces the likelihood of unwanted side reactions such as aromatic ring saturation or coke formation[44].

The preparation method of bimetallic catalysts also plays a critical role in determining their structure and performance. Techniques such as co-impregnation, sequential impregnation, sol–gel synthesis, and hydrothermal crystallization are commonly employed to control the distribution and interaction of metal species. A homogeneous dispersion of metal nanoparticles and the formation of alloy phases are often correlated with superior catalytic properties. In addition, in situ reduction treatments can be used to activate metal species and promote alloy formation, which is essential for achieving the desired catalytic behavior[45].

The support material further influences the performance of bimetallic catalysts. Acidic supports such as zeolites, γ-Al_2O_3, and SBA-15 contribute to C–O bond cleavage, stabilize metal particles, and may participate in proton-transfer mechanisms. When combined with bimetallic sites, these supports enable bifunctional catalysis, where both hydrogenation and acid-catalyzed reactions proceed in a cooperative manner. This is particularly effective in lignin-derived molecules containing both aldehyde and methoxy functionalities[46].

Several studies have reported enhanced HDO performance using Ni–Fe systems. For example, Ni–Fe supported on H-ZSM-5 or mesoporous silica has shown high selectivity toward creosol and guaiacol derivatives, with significant suppression of ring hydrogenation and coke formation. Moreover, bimetallic catalysts exhibit greater thermal and structural stability compared to their monometallic counterparts, making them suitable for long-term operation and regeneration cycles[47].

Table 1.4: Catalytic Performance for HDO of vanillin: Conversion, Selectivity, and Main products under various conditions.

Catalyst	Reaction Conditions (Temperature, Pressure, Solvent)	Conversion (%), Time (h)	Main Product	Selectivity (%)
$Ni/SiO_2–ZrO_2$	573 K, 5 MPa, Octane	100 (16h)	Hydrocarbons	54
Co/N–C	453 K, 1 MPa, 2-propanol	95 (4h)	Creosol	96
Co/N–C	423 K, 1 MPa N2 , 2-propanol	98 (4h)	Creosol	85
$CoMo / Al_2O_3$	573 K, 5 MPa, Dodecane	53 (4h)	Guaiacol	23
Mo_2C	453 K, 1 MPa, Water	100 (3h)	Creosol	78
Pd/C	373 K, 1 MPa, Octane-Water	> 99 (3h)	Creosol	94
Pd/CN	343 K, 1 MPa, Water	99 (1h)	Creosol	98
Ru/CNT	423 K, 1 MPa, Decalin - Water	100 (3h)	Creosol	96
Ru/C	328 K, 1.38 MPa, Water	95 (1h)	Vanillyl Alcohol	91
Au/CNT	423 K, 1 MPa, Decalin	94 (6h)	Creosol	100
$RuCl_3$/TPPTS	343 K, 4.5 MPa, Water - n-hexane	84 (3h)	Creosol	95
$RuCl_2(PPh_3)_3$	363 K, 3.3 MPa, Ethyl Acetate	91 (6h)	Vanillyl Alcohol	72
Ru-Based Shvo	418 K, 1 MPa, Toluene	98 (1h)	Vanillyl Alcohol	91
$Cu–Ni/CeO_2–SiO_2$	433 K, 2.5 MPa, Water	96(12h)	Creosol	82
Cu_3Pd@BBA–1	413 K, 1.0 MPa, 2-propanol	99(8h)	Creosol	94
Co_xP@POP	423 K,4.0 MPa, 2-propanol	100(5h)	Creosol	65

2.5 Zeolite-Supported Catalysts in Biomass Upgrading:

Zeolites have emerged as highly effective support materials in biomass upgrading due to their unique structural features, tunable acidity, high thermal stability, and shape-selective properties. These crystalline microporous aluminosilicates are composed of a three-dimensional framework of SiO_4 and AlO_4 tetrahedra, forming well-defined channels and cavities. Their porous architecture, combined with the presence of Brønsted and Lewis acid sites, makes zeolites particularly well-suited for catalytic applications involving complex oxygenated biomass-derived molecules[48].

In the context of hydrodeoxygenation (HDO), zeolite-supported catalysts play a dual role: they act as supports for active metal species and simultaneously contribute to acid-catalyzed reactions, such as C–O bond cleavage, dehydration, isomerization, and demethoxylation. The integration of metallic and acidic functionalities within a single material allows for bifunctional catalysis, which is essential for promoting selective transformations while suppressing side reactions such as polymerization and coke formation[5].

Several types of zeolites, including H-ZSM-5, Beta(β), Gamma (γ), and Mordenite, have been extensively studied in biomass conversion processes. Among them, H-ZSM-5 has gained particular attention due to its moderate-to-strong acidity, shape selectivity, and high hydrothermal stability. Its pore system (5.5 Å) is ideal for accommodating small-to-medium-sized biomass-derived molecules like vanillin, guaiacol, and furfural, facilitating access to the active sites while minimizing undesired large-molecule reactions that lead to coke[49].

The deposition of metals such as Ni, Fe, Co, and Cu onto zeolite frameworks further enhances catalytic performance. These metals introduce hydrogenation and hydrogenolysis functionalities, enabling the selective removal of oxygen-containing groups under a hydrogen atmosphere. For example, Ni–Fe supported on H-ZSM-5 has shown significant potential in vanillin HDO, selectively converting the aldehyde group to creosol while preserving the aromatic ring structure. The metal–acid synergy promotes sequential hydrogenation and deoxygenation, resulting in efficient product formation with minimal by-products.

The method of incorporating metal species onto zeolites affects the dispersion, reducibility, and interaction between the metal and the support. Common approaches include incipient wetness impregnation, ion exchange, and in situ crystallization or encapsulation. Among these, encapsulation within the zeolite framework has been shown to enhance metal stability, prevent agglomeration, and maintain accessibility to reactants. Moreover, the confinement effect within the microporous network can direct reaction pathways by stabilizing key intermediates[50].

However, the microporous nature of zeolites can also impose diffusional limitations, particularly when processing larger lignin-derived compounds. To address this, hierarchical zeolites, which combine micro- and mesoporosity, have been developed. These materials provide improved molecular transport and accessibility to active sites, leading to enhanced catalytic efficiency and reduced coke formation. Additionally, modifications such as dealumination, desilication, or ion exchange with rare earth or alkali metals can be employed to fine-tune the acidity and structural characteristics of zeolites for specific reaction requirements.

2.6 Solvent Effects in Hydrodeoxygenation Reactions:

The choice of solvent plays a pivotal role in determining the efficiency, selectivity, and overall outcome of hydrodeoxygenation (HDO) reactions, particularly when converting complex oxygenated compounds derived from lignin. Solvents not only serve as a medium for dispersing reactants and facilitating heat and mass transfer, but also influence reaction thermodynamics, hydrogen solubility, catalyst stability, and product distribution. As such, solvent selection is a key parameter in the rational design of catalytic biomass conversion systems[28].

Broadly, solvents used in HDO processes can be classified into protic solvents (e.g., water, alcohols) and aprotic solvents (e.g., THF, 1,4-dioxane). Among these, alcohols—particularly isopropanol (IPA), ethanol, and methanol—are widely employed due to their dual function as solvents and hydrogen donors. In transfer hydrogenation systems, isopropanol is of particular interest, as it can participate in in situ hydrogen generation through dehydrogenation, providing an alternative to molecular hydrogen gas in mild-pressure systems[27].

Isopropanol has been frequently reported as an effective solvent for the HDO of vanillin and related lignin monomers. Its advantages include low toxicity, good hydrogen-donating ability, and compatibility with metal catalysts such as Ni, Fe, and Pd. Moreover, it contributes to suppressing side reactions like condensation and polymerization by stabilizing intermediates and reducing acid-catalyzed degradation pathways. Studies have shown that vanillin dissolved in isopropanol can undergo efficient hydrogenation of the aldehyde group to vanillyl alcohol, followed by deoxygenation to creosol, under moderate temperature and pressure conditions[34,36].

In addition to alcohols, aqueous media have also been explored, particularly when water-tolerant catalysts or hydrothermal conditions are used. However, water can sometimes lead to catalyst deactivation due to metal leaching or hydrolysis of the support. Conversely, aprotic solvents, such as THF and 1,4-dioxane, offer good solubility for aromatic substrates but lack the hydrogen-donating capacity, making them more suitable for systems relying on external hydrogen gas.

The polarity and protic/aprotic nature of the solvent also affect the adsorption and desorption behavior of reactants and products on catalyst surfaces. Polar protic solvents can enhance the solvation of oxygenated intermediates and influence the acid-base interactions between the catalyst support and the substrate. Additionally, solvent molecules may compete with reactants for active sites, thus altering the kinetics and selectivity of the transformation[51].

Table 1.5: Comparison of Catalysts for Hydrodeoxygenation (HDO) of Vanillin: Reaction Conditions, Conversion, Main Products, and Selectivity

Solvent	Solvent characteristics	Mechanism of action	Yields (wt% of lignin)	Advantages	Drawbacks
Water	High dielectric constant	Hydrogen bonding with non-polar solute	39–79	Increasing the density with supercritical conditions can improve solvation	Dynamic equilibrium of solute can alter dissolution
Alcohols	Good solvent polarity index	Rapid dissolution of active species	54–85	Better molecular sources of active H_2	Do not act on all the lignin linkages
Tetralin	Excellent hydrogen donor	Capping of reactive sites	11–40	Help avoid safety hazards of gaseous H_2	Solvent degradation at high temperatures
Formic acid	Supplies H_2 during solvolysis	Provides H_2 through thermal decomposition	72–88	Active at relatively lower temperatures	Forms gaseous products at very high temperatures (~400 °C)

Furthermore, solvent–catalyst interactions can modulate the electronic environment of metal active sites, impacting the activation energy of key steps such as C=O hydrogenation or C–O bond cleavage. In bimetallic systems, solvents may also influence the alloy structure or promote surface restructuring during reaction.

CHAPTER 3: MATERIALS AND METHODS

3.1 Chemicals and Reagents:

Table 3.1: List of chemicals used in Catalyst synthesis & HDO reaction

Sr. No.	Chemical & Reagents	Brand
1.	Nickel (II) nitrate hexahydrate ($Ni(NO_3)_2.6H_2O$)	Sigma Aldrich
2.	Tetra propyl ammonium bromide (TPABr) (98%)	Sigma Aldrich
3.	Chromatographic grade Silica gel (60–120 mesh)	Sigma Aldrich
4.	Sodium hydroxide (NaOH) pellets (≥97.0%)	Merck
5.	Iron nitrate nonahydrate	Sigma Aldrich
6.	Sulphuric acid (98%) (H_2SO_4)	Sigma Aldrich
7.	Sodium Aluminate (Na_2AlO_3)	National Chemicals
8.	Vanillin (≥99.0%)	Sigma Aldrich
9.	2-Propanol (≥99.5%)	Sigma Aldrich
10.	Acetone (≥99.5%)	SRL
11.	N_2 Gas	-
12.	Pyridine (≥99.5%)	Sigma Aldrich
13.	Deionized water (Millipore)	-
14.	Ammonium sulphate $(NH_4)_2SO_4$	Sigma Aldrich

3.2 Experimental:

3.2.1 Catalyst Preparation

3.2.1a Synthesis of HZSM-5:

The synthesis of the H-ZSM-5 (Si/Al ratio = 41.6) was performed according to the procedure described by Rollmannn et al.[52]. Some modifications were made to the process: For the first solution, 25 ml of silica sol was prepared by adding 0.15 moles of

chromatographic grade silica gel and 0.0625 mol of NaOH into 25 ml of deionized water. The mixture was stirred at 60–70°C until it turned into a silica solution. For the second solution, 0.0036 moles of $NaAlO_2$ was dissolved in 25 ml of deionized water. For the third solution, 0.015 moles of TPABr and 0.030 mol of (96%) H_2SO_4 were dissolved in 50 ml of deionized water. The second and third solutions were mixed with the first solution and vigorously stirred for 5-10 minutes. Then, the pH was adjusted to between 11 and 12, and the final solution was left for a further 30 minutes, stirring until the gel formed. It was then poured into a polypropylene narrow-mouth screw cap bottle. The bottle was tightly closed and placed in an oven at 95°C for five days. The solid crystallized product was observed after five days of aging. It was washed with an excess of deionized water until the pH of the washing became neutral. The calcination of the product was performed at a rate of 4°C/min up to 100°C, and then the rate was increased to 10°C/min to 500°C, where it was kept for 3 hours to remove the organic template (TPABr) to obtain Na-ZSM-5. The ammonia exchange of the calcined product (Na-ZSM-5) was performed with 0.1M $(NH_4)_2SO_4$ solution (10 ml/gm) for 20 minutes at ambient temperature. It was then washed, dried, and again calcined at 500°C for 3 hours to obtain HZSM-5.

3.2.2b Synthesis of Ni_xFe_y@HZSM-5 Catalysts:

The Fe_xNi_y @ H-ZSM (10%) catalyst were prepared by the incipient impregnation method. Firstly, 350mg H-ZSM was weighed and put into a beaker containing 50 ml deionized water. Secondly, ferric nitrate and nickel nitrate were added to the dispersed H-ZSM-5 suspension, and kept magnetically stirring at 500 r/min at room temperature for 24 h, then the sample were dried and calcined in a muffle furnace at 550 ^{0}C for 5 h. Regarding the selection of metal sources, it should be noted that the source for loading iron and nickel metals should not be nitrate, in order to avoid residual N participating in the reaction during HDO. Lastly, the sample were reduced at 300 ^{0}C for 3 h under 5 MPa H_2 pressure in an autoclave reactor to obtain the FexNiy@H-ZSM-5 (10%) catalyst, where x/y was the molar ratio of Fe/ Ni and 10 % was the mass content, respectively. The synthesis process of catalyst Fe_xNi_y @HZSM-5 was shown in figure 3.2.

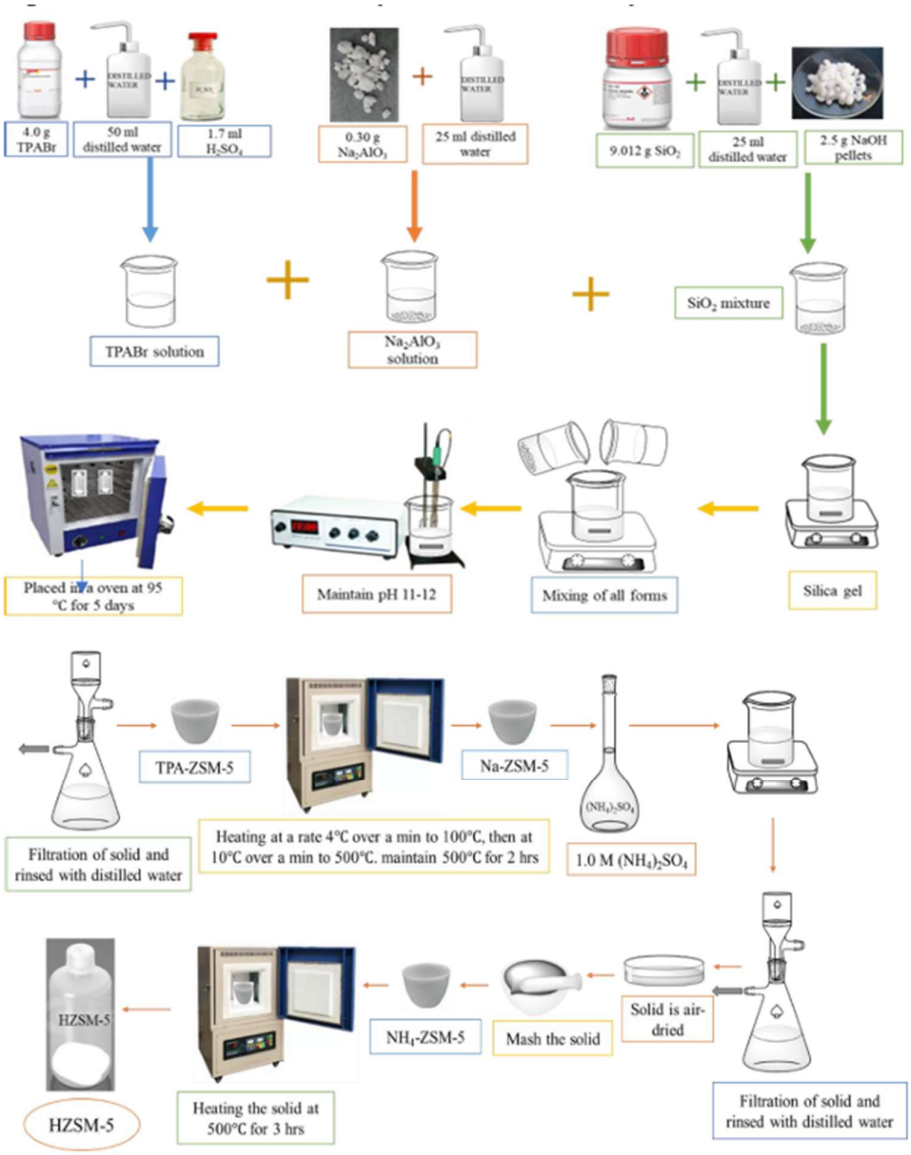
4.0 g TPABr
50 ml distilled water
1.7 ml H_2SO_4
0.30 g Na_2AlO_3
25 ml distilled water
9.012 g SiO_2
25 ml distilled water
2.5 g NaOH pellets
TPABr solution
Na_2AlO_3 solution
SiO_2 mixture
Placed in a oven at 95 °C for 5 days
Maintain pH 11-12
Mixing of all forms
Silica gel
Filtration of solid and rinsed with distilled water
TPA-ZSM-5
Heating at a rate 4°C over a min to 100°C, then at 10°C over a min to 500°C. maintain 500°C for 2 hrs
Na-ZSM-5
$(NH_4)_2SO_4$
1.0 M $(NH_4)_2SO_4$
Filtration of solid and rinsed with distilled water
Solid is air-dried
Mash the solid
NH_4-ZSM-5
Heating the solid at 500°C for 3 hrs
HZSM-5
HZSM-5

Figure 3.1: An overview of the synthesis of HZSM-5 support

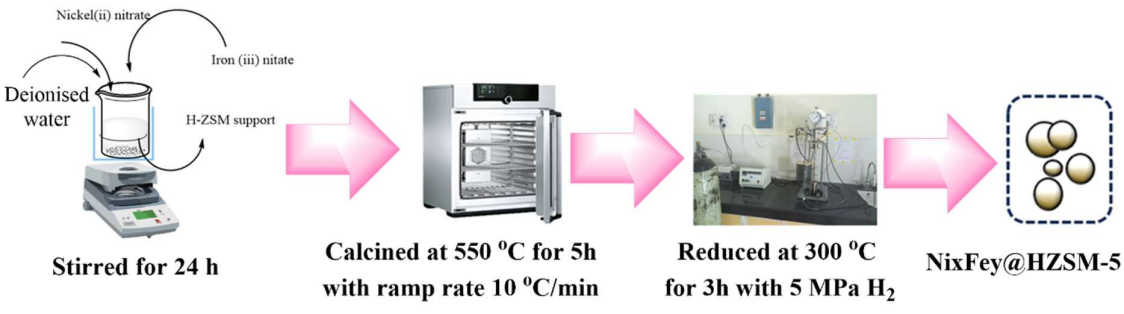
Nickel(ii) nitrate
Iron (iii) nitate
Deionised water
H-ZSM support
Stirred for 24 h
Calcined at 550 °C for 5h with ramp rate 10 °C/min
Reduced at 300 °C for 3h with 5 MPa H_2
NixFey@HZSM-5

Figure 3.2: Schematic Representation of Synthesis of NixFey@H-ZSM-5 catalysts

3.3 Catalyst Characterization

The following are the catalyst characterization techniques

➢ XRD: Catalyst crystal structure characterization.

➢ SEM-EDS: External morphology of the catalyst and elemental composition.

➢ BET-BJH: Surface area and pore size of the catalyst.

➢ FTIR: Functional Group changes in reaction products

➢ TG-DTA:- Thermal stability, checking coke formation on the catalysts

3.3.1 Powder X-ray Diffraction (PXRD) Analysis

The PXRD technique is a very important experimental analysis tool used to determine the phase identification of chemical compounds, the crystal structure and the lattice parameter with geometry of the solid compounds. The PXRD techniques are highly used to determine the polymorph, stability of drug compounds, Creation, and validation of a method for drug identification and quantification in the pharmaceutical industry. In XRD, the beam of X-rays wavelength ranging from 0.7 to 2 Å is incident on the specimen and is diffracted by the crystalline phases in the specimen. According to W. L. Bragg diffraction patterns can be explained in terms of reflections from the inner crystal planes, which form a continuous spectrum of the incident radiation. This scattered X-ray amplitude will superpose and form give rise constructive and destructive interference producing a diffraction pattern. This diffraction of angles equal to the Bragg angle.

$n\lambda = 2d_{hkl} \sin\theta$

Where n is the integer(1, 2, 3…) called the order of reflection, d_{hkl} is termed as the interplanar spacing between the crystalline plane in the solid phase, λ is the X-ray wavelength, θ is the glancing angle of incident X-rays and crystal plane. The diffracted X-ray wavelength and its intensity are measured as a diffraction angle 2θ and the specimen orientation. The X-ray diffractometer design in such a way that the samples holder rotates in the X-ray beam's path with an angle θ while the detector rotates to collect the diffracted X-ray at an angle 2θ. For common and regular powder patterns, the data were collected at 2θ from 5° to 70° angles present in the X-ray scan. The obtained diffraction pattern is used

to identify the sample crystalline phases, crystal structure with its parameter, and to measure its structural properties. The PXRD is a non-destructive characterization technique used to identify the nanoparticles, and a good approximation of their particle size, also able to find using Scherrer's formula167. The XRD pattern is used to identify the pharmaceutical co-crystal, which gives the confirmation of co-crystal formation168. The instrumentation and basic principle was shown in Figure 3.3.

Powder diffraction data were collected using the Bruker Advance D8, Eco X-ray diffractometer (Figure 3.3), Ni filtered CuK=1.54056 radiation, and Lynxeye detector at 25 mA and 40 kV radiation. At room temperature, the data were taken using a Si zero-background sample holder. The dispersed intensities were calculated using a scintillation counter. The angular distance (2θ), measured in 0.02° steps, ranged from 5° to 90°, and the measuring duration was 0.3 seconds for each step. The data was examined using the Bruker suite of programs and the Diffract. Eva and TOPAS programs. PXRD analysis was performed to determine if any variations in their XRD pattern could indicate the affect loading of metals on H-ZSM-5.

Figure 3.3: XRD Instrument

3.3.2 SEM

Scanning electron microscopy (SEM) was performed using a JEOL(JSM-7500F) instrument(Figure 3.4) to determine the catalyst's surface morphology. Scanning electron microscope conducted at 5.0 kV, SEM-FEG apparatus equipped with an energy dispersive spectrometer (EDAX). EDAX was used to determine uniform dispersion of elements on the surface of the catalyst and their composition in the form of %.

Figure 3.4: SEM Instrument

3.3.3 BET

Stephen Brunauer, Paul Emmett, and Edward Teller introduced the BET theory in 1938. The BET theory built upon Irving Langmuir's 1916 Langmuir theory. The Langmuir hypothesis posits a link between the gas pressure just above a solid surface and the monolayer adsorption of gas molecules on a solid surface (also known as adsorbates). It's called adsorption when gas molecules stick to the surface of a material. Absorption, on the other hand, occurs when a liquid or solid absorbs a fluid. Surface area, temperature, gas pressure, and strength of the gas solid interaction all influence the amount of gas adsorbed. Nitrogen is employed in BET surface area analysis because it is available in large purity and has a strong interaction like most solids. For a BET isotherm, the amount of gas adsorbed versus relative pressure is represented graphically by the data170. While direct

measurement of an amorphous porous material's surface or geometrical area is highly challenging, a crystalline porous material's atomic structure is accessible for experimentation, allowing for individual calibration of the BET area. The BET method is extensively used to evaluate nanostructured materials' large specific surface area. The basic instrumentation is given in Figure 3.5.

Figure 3.5: BET Instrument

3.3.4 FTIR

In the realm of membrane application, the use of FTIR analysis is critical to justifying changes in their characteristics and performance in diverse applications. A spectrophotometer is an instrument that determines a compound's absorbance spectrum. When compared to a typical spectrophotometer, the Fourier transform spectrophotometer will provide an Infrared spectrum faster. For all frequencies, the indicator measures the particular interferogram signal in energy against time. Interferograms remove the sample spectrum's background spectrum automatically with computer software called Fourier processing. FTIR analysis uses the term absorption when a photon moves toward a molecular structure and causes it to rise in energy. This is due to excited states in the IR region of light spectrum which cause the molecular bond vibrations (stretching, bending and twisting) as well as out-of-plane deformation. It is these intrinsic physical and

chemical properties that dictate the IR absorbance peak wavenumber, which acts as an identification fingerprint for each functional group for example C–H, O–H, C=O.

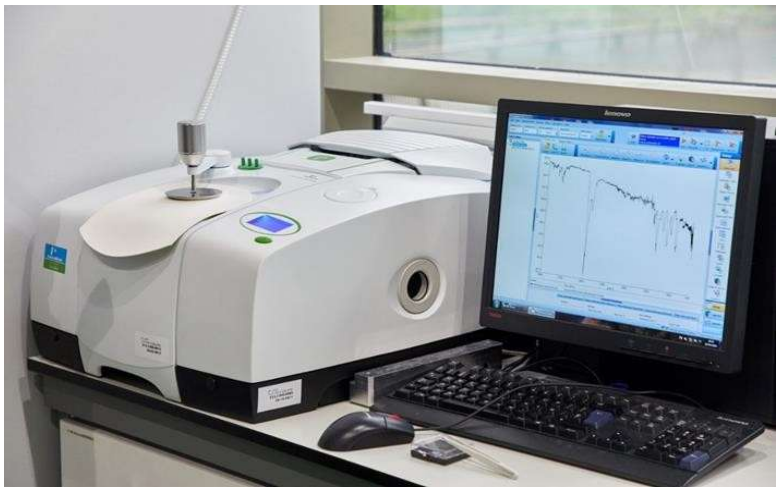

Figure 3.6: FTIR Instrument

3.3.5 TG-DTA

Thermogravimetric analysis (TG) and differential thermal analysis (DTA) are thermal techniques used to study the weight changes and thermal behavior of materials as a function of temperature. In this study, TG–DTA was performed to evaluate the thermal stability and decomposition profile of the synthesized Ni–Fe@HZSM-5 catalysts. This analysis helps to determine the removal of moisture, decomposition of metal precursors (such as nitrates), and the suitable calcination temperature required for catalyst activation. The TG curve shows the weight loss pattern, while the DTA curve indicates whether the associated changes are exothermic or endothermic in nature. These results are important to ensure that the catalyst is thermally stable and properly activated before being used in the hydrodeoxygenation reaction.

3.4 Catalytic Reaction:

All Experiments were conducted in a 50 mL stainless steel SS316 (Parr Instruments Co., Illinois, USA) high-pressure close batch reactor. The reactor was purged with nitrogen twice or more to remove air. Typically, 1 mmol of Vanillin, 50 mg of catalysts, and 25 mL of isopropyl alcohol (IPA) were mixed and added into 50 mL stainless steel closed batch reactor, which was sealed and elevated to a specific reaction temperature at 1000 rpm. After the proper reaction time, the reactor was quenched to RT. The reaction mixture were filtered and analysed by Gas chromatography-mass spectrometry (GC-MS).

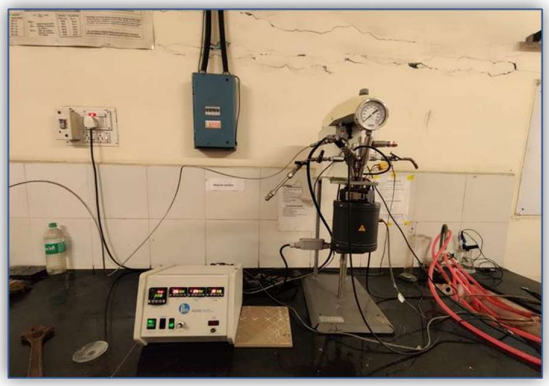

Figure 3.5: Close-batch reactor (Parr Illinios)

3.4a Sample Analysis:

Qualitative identification of products was conducted on a gas chromatography-mass spectrometer apparatus (GC-MS; Agilent 5977A MSD; Agilent MS NIST library) equipped with an HP-5 MS capillary column (30 m × 250 µm × 0.25 µm). The initial temperature (60°C) was held for 0 min, then heated at 10°C.min^{-1} to 230°C, and held for 5 min. Quantitative analysis of products was performed on an Agilent GC-7890B equipped with a flame ionization detector (GC-FID) employed as the same temperature program and capillary column DB-5 (30 m × 250 µm × 0.16 µm) as described for GC-MS. The conversion of LA, the selectivity of GVL, and the yield of GVL were calculated using the equations listed below.

$$\textit{Conversion (\%)} = \left(\frac{\textit{Actual moles of VAN reacted}}{\textit{Initial moles of VAN}}\right) \times 100 \quad \text{.....(1)}$$

$$Yield\ of\ Creosol\ (\%) = \frac{Moles\ of\ Creosol\ in\ products}{Initial\ moles\ of\ VAN} \times 100 \ldots\ldots\ldots\ldots\ldots\ldots\ldots\ldots\ldots\ldots (2)$$

$$Selectivity\ (\%) = \frac{Moles\ of\ Creosol\ product}{Total\ moles\ of\ VAN\ reacted} \times 100 \ldots\ldots\ldots\ldots\ldots\ldots\ldots\ldots\ldots\ldots\ldots\ldots\ldots\ldots (3)$$

Figure 3.6: GC-MS & GC-FID Instrument

3.4b Calibration Curve Analysis

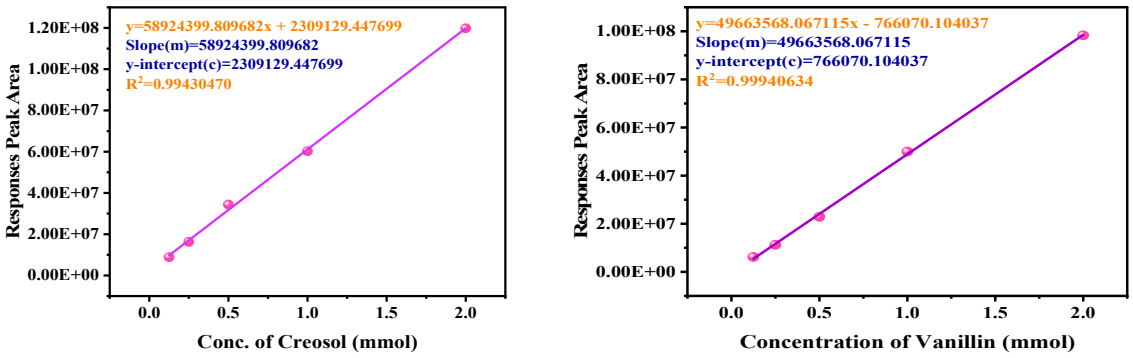

Figure 4.9 Calibration curve of Creosol and vanillin

The above calibration equations were applied to quantify the concentrations of vanillin and creosol in post-reaction samples by substituting the experimental peak area values into the respective equations. These concentrations were then used to calculate: (a)Vanillin conversion (%) (b) Creosol yield (%).

3.5 Optimization Studies

A series of optimization studies were conducted to determine the ideal reaction conditions. The following parameters were varied one at a time while keeping others constant:

1. Catalysts Screening: Ni:Fe molar ratio: 1:1, 1:2, 1:3 2:1, 3:1 & 3:2.

2. Catalyst dosage: 10, 20, 30, and 40 % wt.
3. Reaction temperature: 160, 180, 200, and 220 °C
4. Reaction time: 3, 6, 9, 12, and 18 h

The effect of each variable on the vanillin conversion and creosol selectivity was studied, and the optimal condition was found to be 30 wt % of Ni2Fe@HZSM-5 catalyst, 200 °C reaction temperature, 12 h reaction time, and 25 mL IPA as the hydrogen donor and solvent.

CHAPTER 4: RESULTS AND DISCUSSION

4.1 Characterization of Catalysts:

4.1.1 PXRD Analysis

PXRD analysis was performed to investigate the structural integrity of the HZSM-5 support after metal impregnation and to assess the crystallinity of the loaded metal species. Figure 4.1 shows the diffraction patterns of pure HZSM-5 and a series of metal-loaded catalysts, including monometallic (Ni@HZSM-5 and Fe@HZSM-5) and bimetallic Ni-Fe combinations at various molar ratios (Ni2Fe, NiFe2, Ni3Fe, NiFe3, and equimolar NiFe).

All samples exhibit well-resolved diffraction peaks characteristic of the MFI structure of HZSM-5, with prominent reflections at 2θ ≈ 7.9°, 8.8°, 23.1°, 23.9°, and 24.3°, corresponding to the (101), (200), (501), (303), and (313) planes, respectively. These peaks remain essentially unchanged after metal loading, indicating that the zeolite framework retains its crystallinity and structural integrity post-impregnation and calcination. This finding is consistent with those of Dayaram et al[53]. (2022), who reported that Ni and Fe loadings on HZSM-5 did not alter the primary diffraction pattern of the parent zeolite, thereby confirming the thermal and chemical robustness of the support.

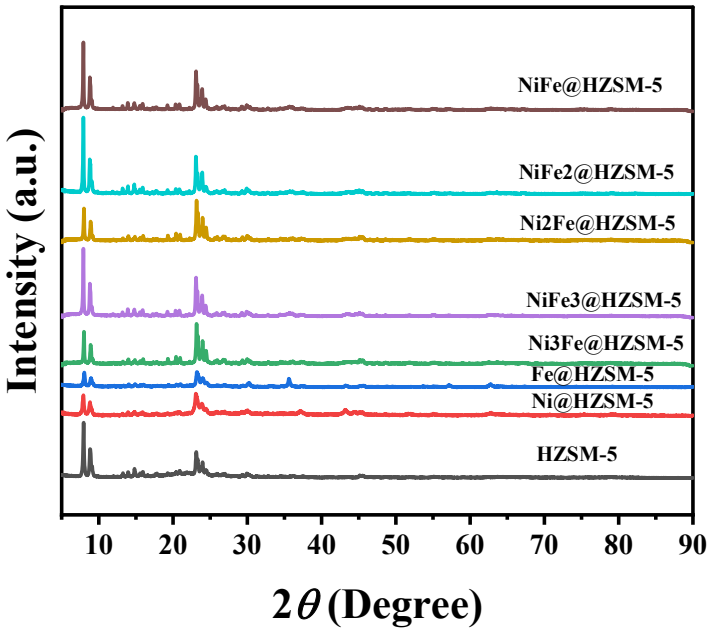

Figure 4.1: XRD pattern for a different molar proportion of Ni & Fe supported HZSM-5.

4.1.2 FTIR Analysis

Fourier-transform infrared spectroscopy (FTIR) was used to investigate the structural integrity and chemical environment of the HZSM-5 zeolite upon incorporation of Ni, Fe, and their combinations. The spectra (Figure 4.2) exhibit characteristic bands of the MFI-type zeolite framework, confirming the retention of the crystalline structure after metal loading.

Key absorption bands at ~1080, 800, and 450 cm^{-1} are assigned to the asymmetric stretching, symmetric stretching, and bending vibrations of the internal Si–O–Al framework, respectively. These bands remain prominent across all samples, indicating the framework integrity of HZSM-5 is preserved upon Ni and Fe incorporation.

The band observed at ~550 cm^{-1}, highlighted in the shaded blue region, is attributed to the five-membered ring vibrations specific to the MFI-type structure. Its persistence suggests no significant framework distortion due to metal loading.

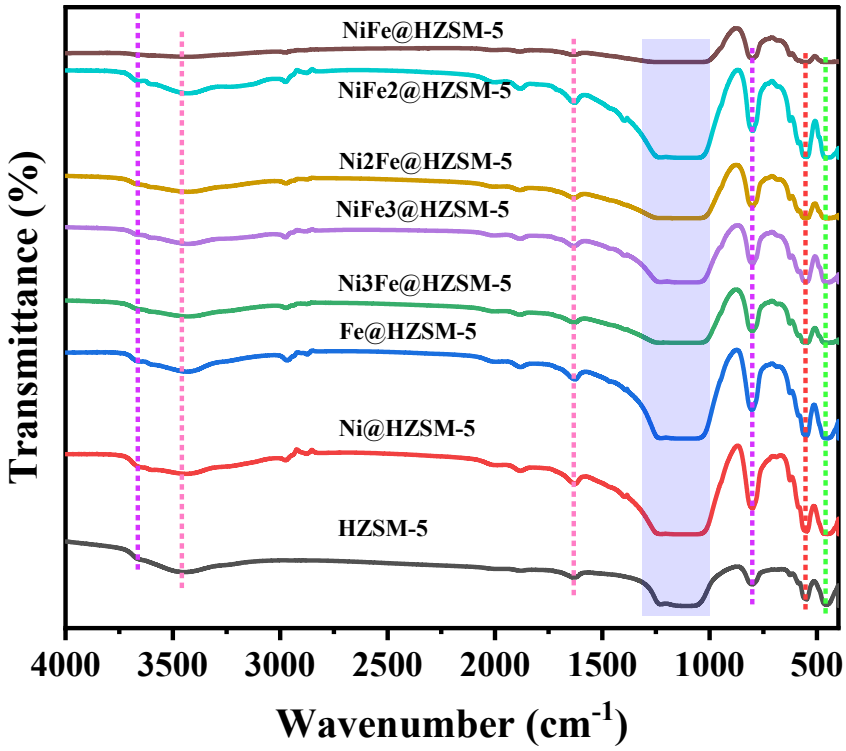

Figure 4.2: FTIR spectrum for a different molar proportion of Ni & Fe supported HZSM-5.

Notably, an additional weak band around 960 cm^{-1} becomes more defined in the metal-loaded samples, particularly in those with higher Fe or Ni content. As reported in the reference paper, this band is indicative of Si–O vibrations perturbed by the presence of extra-framework metal species or Si–OH groups resulting from partial dealumination or framework modification. The increased intensity of this band suggests successful incorporation or interaction of Ni^{2+} and Fe^{3+} species with the zeolite framework or surface hydroxyls.

The broad absorption bands around 3450 cm^{-1} and a smaller peak near 1630 cm^{-1} are associated with the O–H stretching and bending vibrations of adsorbed water, respectively. The relative intensity of these bands varies with metal content, possibly due to changes in hydrophilicity or the number of accessible hydroxyl groups on the catalyst surface.

Additionally, a small but distinguishable peak at ~793 cm^{-1} in the Ni-loaded samples is consistent with Ni–O stretching vibrations, supporting the presence of nickel oxide species as previously noted in similar studies.

4.1.3 SEM-EDS

The morphology of the HZSM-5 and HZSM-5 supported Ni-Fe bimetallic (Ni2Fe@HZSM-5) catalyst was determined by scanning electron microscopy. Figs 4.3 (a-d) shows the SEM micrographs of the HZSM-5, while (e-h) display the SEM micrographs of the Ni2Fe@HZSM-5 catalysts. The SEM analysis of the HZSM-5 sample indicates that the particles are roughly spherical in morphology with porous surfaces. Fig 4.3 (i) presents the EDS spectrum of Ni2Fe@HZSM-5, showing that approximately 8% weight loading of metals is present on the surface of HZSM-5.

The surface morphology and elemental composition of the synthesized catalysts were investigated using scanning electron microscopy (SEM) and energy-dispersive X-ray spectroscopy (EDS). Fig. 4.3 (a–d) shows the SEM images of the parent HZSM-5 catalyst, while Fig. 4.3 (e–h) presents the SEM images of the Ni2Fe@HZSM-5 catalyst at various magnifications. The HZSM-5 sample exhibits well-defined crystalline particles with a relatively uniform size distribution and typical roughly spherical morphology, characteristic of ZSM-5 zeolite. The surface appears clean and free of any agglomerated particles.

Upon loading Ni and Fe metals, the SEM images of Ni_2Fe@HZSM-5 reveal noticeable surface roughening and the appearance of small dispersed particles on the external surface, indicating successful deposition of the metal species. No significant agglomeration is observed, suggesting good dispersion of Ni and Fe on the support. The particle size distribution shown in Fig. 4.3 (j) indicates an average particle size in the 163 μm range, consistent with the expected size range for bimetallic nanoparticles supported on zeolites.

The EDS spectrum of Ni2Fe@HZSM-5 (Fig. 4 .3i) confirms the presence of Ni and Fe along with Si, Al, and O elements originating from the zeolite framework. The successful detection of Ni and Fe peaks validates the incorporation of these metals into the zeolite matrix. Furthermore, elemental mapping (Fig. 4.3 k) reveals a uniform distribution of Ni and Fe throughout the HZSM-5 support. This indicates that the bimetals are well dispersed over the zeolite surface without noticeable clustering or segregation

Overall, the SEM-EDS analysis confirms that the morphology of HZSM-5 is preserved after metal loading, and the Ni and Fe species are homogeneously distributed, which is beneficial for ensuring high accessibility of active sites during catalytic reactions

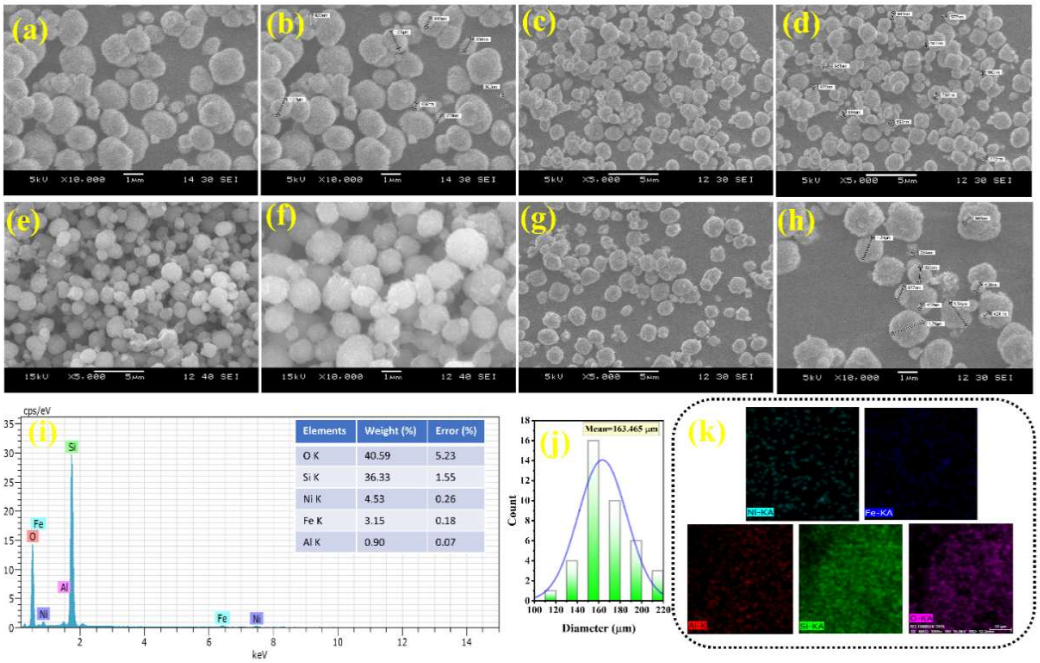

Figure 4.3: SEM images of HZSM-5 (a-d), SEM images of Ni2Fe@HZSM-5 (e-h), EDS Spectrum (i), Average Particle size (j), and Elemental mapping (k) of Ni2Fe@HZSM-5

4.1.4 N_2- Adsorption Desorption

The Brunauer-Emmett-Teller (BET) analysis was utilised to measure surface area, average pore size, and pore volume of the as-synthesized catalysts (Figure 4.4). The Brunauer–Emmett–Teller (BET) surface area, pore volume, and average pore radius of the samples are summarized in Table 4.1. The N_2 adsorption-desorption isotherm analysis (BET-BJH) of HZSM-5 and Ni2Fe@HZSM-5 shows a type IV characteristic isotherm with a prominent H2 hysteresis loop at low pressure ($p/p_o<0.42$), which indicates the microporous nature of the samples, which is typical for zeolites (Figure 4.4a, b). The surface area of the as-synthesized catalysts was analysed using multipoint BET plots (Figure 4.4c, d). The surface area plot shows an increase in nitrogen adsorption for HZSM-5 and Ni2Fe@HZSM-5 with the steady increase in the relative pressure. The parent HZSM-5 exhibited a high BET surface area of 343.861 m^2/g, a total pore volume of 0.0736 cm^3/g, and an average pore radius of 1.88 nm. A noticeable reduction in surface area was observed upon the incorporation of Ni and Fe metals via bimetallic loading. The BET surface area of Ni2Fe@HZSM-5 decreased to 227.8 m^2/g. This reduction can be attributed to the partial blockage of micropores and mesopores of the HZSM-5 framework by metal species during the impregnation and calcination process. Interestingly, the total pore volume increased to 0.0898 cm^3/g, while the average pore radius slightly decreased to 1.63 nm. The increase in pore volume, despite the lower surface area, may result from the generation of new mesopores or interparticle voids due to the deposition of metal nanoparticles on the external surface or at the pore mouths, disrupting the original microporous structure. The slight reduction in pore radius further supports the hypothesis that metal species have partially occupied the microporous channels of HZSM-5.

Table 4.1 Physicochemical properties (BET surface area, pore volume, & pore radius) of HZSM-5 and Ni2Fe@HZSM-5.

Entry	Catalysts	BET surface area (m^2/g)	Pore Volume (cm^3/g)	Pore radius (nm)
1	HZSM-5	343.861	0.0735919	1.87887
2	Ni2Fe@HZSM-5	227.8	0.0897716	1.63225

Overall, the N_2 physisorption results confirm the successful loading of NiFe bimetals onto HZSM-5 and the associated modification of its porous structure, which may influence the catalytic activity and diffusion properties of reactants and products during the reaction.

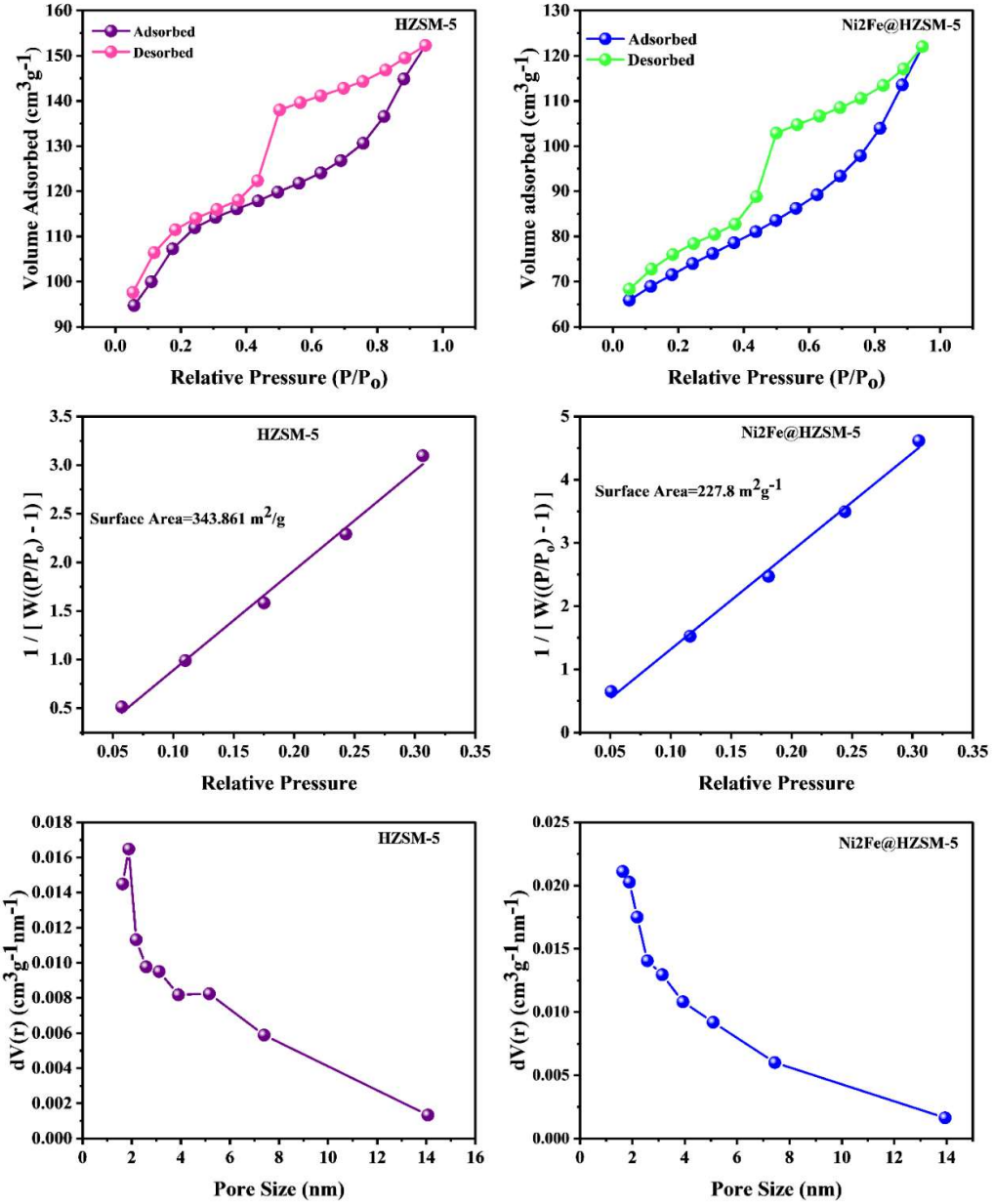

Figure 4.4: BET plots of (a,b) N_2 adsorption-desorption isotherms, (c,d) Surface area plots, and (e,f) BJH pore size distribution plots of HZSM-5 and Ni2-Fe@HZSM-5

4.1.5 Thermogravimetric Analysis (TGA)

Thermogravimetric analysis (TGA), differential thermogravimetric (DTG), and differential thermal analysis (DTA) were carried out to investigate the thermal stability and decomposition behavior of the unmodified HZSM-5 support and the bimetallic Ni2Fe-loaded HZSM-5 catalyst. The results are presented in Figure 4.5, showing mass loss (TGA), derivative weight loss (DTG), and thermal effects (DTA) as a function of temperature under a nitrogen atmosphere.

The TGA curves of both HZSM-5 and Ni2Fe@HZSM-5 exhibit distinct weight loss steps, which can be attributed to different thermal events. For HZSM-5, the first weight loss (~3–4%) occurs below 150 °C, which is attributed to the removal of physisorbed water and volatile impurities. No significant mass loss is observed beyond 150 °C, indicating high thermal stability of the zeolite framework in the absence of metal loading. For Ni2Fe@HZSM-5, an initial weight loss below 150 °C (~2–3%) is also due to moisture desorption. A second weight loss (~5–7%) occurs in the range of 200–450 °C. This is likely associated with the decomposition of residual organic moieties or nitrate species from the metal precursors (e.g., $Ni(NO_3)_2$ and $Fe(NO_3)_3$). The total weight loss observed for Ni2Fe@HZSM-5 is higher than that of pure HZSM-5, confirming the successful incorporation of metal species and their thermal decomposition behavior.

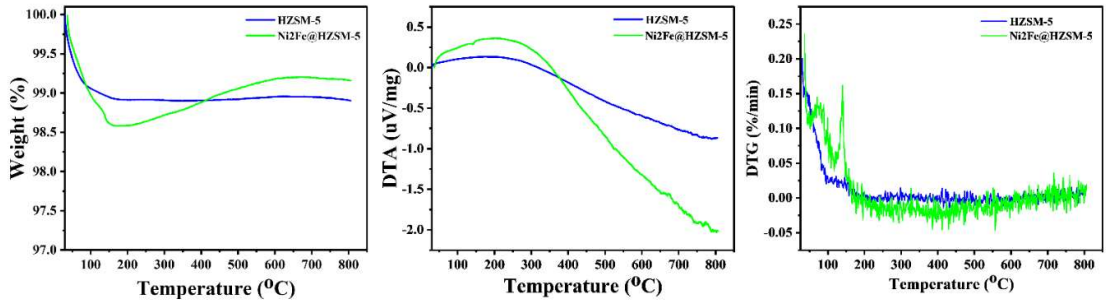

Figure 4.5: Thermal properties of HZSM-5 & Ni2-Fe@HZSM-5 (a) TGA (b) DTG (c) DTA

The DTG curve for HZSM-5 shows a broad and shallow peak below 150 °C, corresponding to the desorption of water. In contrast, the DTG profile of Ni2Fe@HZSM-5 exhibits two distinct peaks: (i) the first at ~110 °C (moisture removal), and (ii) the second around ~350 °C, which indicates the thermal decomposition of metal precursor residues

and possible transformation of metal oxides. The DTA signal supports these observations: (i) for HZSM-5, only a small endothermic peak is observed at low temperature (~100 °C), and (ii) for Ni2Fe@HZSM-5, a pronounced endothermic peak is seen at ~350 °C, aligning with the DTG peak and further confirming the decomposition of metal-containing species.

4.2 Catalyst Screening and Optimization

The catalytic hydrogenation of vanillin to creosol is a complex, multi-step transformation that requires the cooperative action of hydrogenation and deoxygenation sites under appropriate thermal and chemical conditions. In this work, a systematic investigation was carried out to screen various mono- and bimetallic catalysts supported on HZSM-5 and to optimize key reaction parameters, including metal composition, reaction temperature, catalyst dosage, and reaction time. The efficiency of each catalyst was evaluated based on vanillin conversion (%) and creosol yield (%), aiming to identify a highly active and selective catalytic system for the valorization of biomass.

4.2.1 Catalyst Composition Screening

Catalyst composition is a critical factor influencing catalytic performance, particularly in bifunctional systems such as bimetallic Fe–Ni catalysts. The performance of several catalysts supported on HZSM-5 was assessed, and the results are summarized in Table 4.1. The parent zeolite HZSM-5, used without any metal incorporation, showed very poor activity, with only 25% vanillin conversion and 5% creosol yield. This limited activity is attributed to the absence of metal sites required for hydrogenation. Although HZSM-5 possesses acidic Brønsted sites that can activate some reaction intermediates, it cannot facilitate the transfer hydrogenation or C–O bond cleavage essential for producing creosol.

The incorporation of transition metals significantly improved catalytic performance. The monometallic Ni@HZSM-5 catalyst exhibited a notable enhancement, achieving 74% conversion and 69% yield, which highlights Nickel's excellent hydrogenation ability. Nickel promotes the reduction of the aldehyde group in vanillin to vanillyl alcohol and potentially facilitates C–O bond cleavage to produce creosol. Similarly, Fe@HZSM-5 exhibited reasonable activity, with 60% conversion and 52% yield, suggesting that iron sites may facilitate deoxygenation reactions, although its hydrogenation capability is relatively weaker than that of nickel.

To explore synergistic effects between Ni and Fe, a series of bimetallic catalysts with varying molar ratios were synthesized. The NiFe@HZSM-5 catalyst (1:1 molar ratio) demonstrated a further improvement in catalytic efficiency, giving 78% conversion and 74% yield. This enhancement suggests a cooperative mechanism in which Ni facilitates hydrogenation while Fe enhances the selective cleavage of the C–O bond. Optimizing the Ni:Fe molar ratio was found to be crucial. The catalyst with a 2:1 Ni:Fe ratio (Ni2Fe@HZSM-5) exhibited the highest catalytic performance with 84% conversion and 80% creosol yield. This composition provided an ideal balance between hydrogenation and deoxygenation activity, suggesting that moderate nickel enrichment ensures sufficient hydrogen activation while retaining the beneficial influence of iron.

However, further increasing the nickel content to produce Ni3Fe@HZSM-5 resulted in a slight decline in performance, with 80% conversion and 74% yield. This may be due to the agglomeration of excess Ni particles or the blockage of zeolite pores, which reduces the active surface area and accessibility. On the other hand, increasing the iron content beyond the 1:1 ratio, as in NiFe2@HZSM-5 and NiFe3@HZSM-5, led to significantly reduced yields (61% and 55%, respectively), likely due to insufficient hydrogenation capacity. These results confirm that Ni2Fe@HZSM-5 exhibits the most desirable catalytic profile for vanillin hydrogenation and was selected for further reaction optimization.

4.2.2 Influence of Reaction Temperature

Temperature plays a vital role in reaction kinetics and product distribution. To evaluate its effect, the Ni2Fe@HZSM-5 catalyst was tested across a temperature range of 160–220 °C. As shown in Table 4.2, vanillin conversion and creosol yield increased with temperature up to 200 °C, reaching 84% conversion and 80% yield. This improvement is attributed to enhanced molecular collisions, better activation of isopropyl alcohol as a hydrogen donor, and accelerated bond-breaking reactions at elevated temperatures.

Interestingly, a further increase to 220 °C resulted in a slight decrease in both conversion (82%) and yield (79%). This decline may be due to competing side reactions, thermal degradation of the product, or over-reduction of vanillin intermediates. Thus, 200 °C was identified as the optimal reaction temperature, providing a balance between reaction rate and product yield.

4.2.3 Influence of Catalyst Dosage

The effect of catalyst loading was examined by varying the amount of Ni2Fe@HZSM-5 from 10 to 40 wt% %. As detailed in Table 4.3, increasing the catalyst dosage from 10 to 30 wt% resulted in a significant improvement in vanillin conversion and creosol yield. At 30 wt%, the reaction achieved an 84% conversion and an 80% yield, indicating sufficient active sites for effective substrate activation and transformation.

However, a further increase to 40 wt% resulted in only a marginal increase in conversion (86%) and a negligible improvement in yield (81%). The diminishing returns suggest that catalyst concentration beyond 30 wt% reaches a saturation point, where mass transfer limitations or catalyst agglomeration may counteract further gains. Therefore, 30 wt% catalyst dosage was selected as optimal for subsequent reactions.

4.2.4 Influence of Reaction Time

Reaction time is another crucial parameter that affects conversion and selectivity. The time-dependent performance of Ni2Fe@HZSM-5 was evaluated over a range from 3 to 15 hours. The data in Table 4.4 demonstrate a gradual increase in both conversion and yield up to 12 hours, at which point maximum performance (84% conversion, 80% yield) was observed. The increase over time reflects the progression of both hydrogenation and deoxygenation pathways.

Extending the reaction to 15 hours resulted in only a minor increase in conversion (86%), while the yield decreased slightly (78%). The decrease in yield after 12 hours suggests possible product instability, secondary reactions, or degradation of creosol under prolonged heating. Hence, 12 hours was determined to be the optimal reaction time, ensuring maximal product formation while minimizing side reactions.

4.2.5 Overall Assessment of Catalytic System

The combined results from catalyst composition and process parameter screening confirm that the Ni2Fe@HZSM-5 catalyst, operating at 200 °C for 12 hours with a 30 wt% catalyst loading, achieves the most efficient conversion of vanillin to creosol. The superior performance of this system is attributed to the synergistic interaction between Ni and Fe, which together facilitate selective hydrogenation and C–O bond cleavage, supported by the acidic framework of HZSM-5 that aids substrate activation and product stabilization.

This optimized catalytic system provides a robust, selective, and sustainable route for the valorization of lignin-derived vanillin into high-value aromatic compounds, such as creosol, thereby supporting the development of green chemical technologies.

Table 4.2: Optimization of Fe–Ni Molar Proportion in Catalyst Composition

Catalyst	Conversion (%)	Yield (%)
HZSM-5	25	5
Ni@HZSM-5	74	69
Fe@HZSM-5	60	52
NiFe@HZSM-5	78	74
Ni2Fe@HZSM-5	84	80
Ni3Fe@HZSM-5	80	74
NiFe2@HZSM-5	72	61
NiFe3@HZSM-5	64	55

Table 4.3: Influence of Catalyst Dosage

Catalyst Dose (Wt%)	Conversion (%)	Yield(%)
10	65	61
20	74	71
30	84	80
40	86	81

Table 4.4: Effect of Reaction Temperature on Product Distribution

Temperature	Conversion (%)	Yield (%
160	48	43

180	62	57
200	84	80
220	82	79

Table 4.4: Influence of Catalyst on Time

Time (hr)	Conversion (%)	Yield (%)
3	32	29
6	46	41
9	65	60
12	84	80
15	86	78

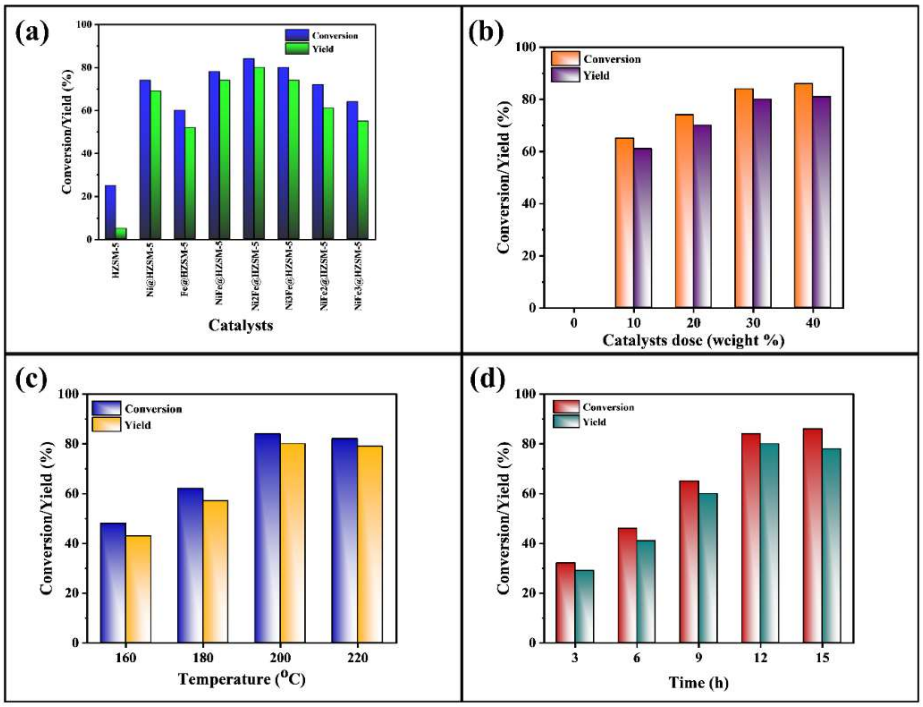

Fig. 4.6 Optimization of reaction conditions for the conversion of vanillin to creosol. (a) Variations in Catalysts (reaction conditions: vanillin=1mmol, IPA=25mL, catalyst

amount=30 wt.%, temperature=200°C, time=12h), (b) Variations of catalyst dose (reaction conditions: vanillin=1mmol, IPA=25mL, catalyst=Ni2Fe@HZSM-5, temperature=200°C, time=12h, (c) Variations of temperature (reaction condition: vanillin=1mmol, IPA=25mL, catalyst amount=30 wt.%, time=12h), (d) Variations of time (reaction condition: vanillin=1mmol, IPA=25mL, catalyst amount=30 wt.%, temperature=200°C.

4.3 Proposed Reaction Pathway

The catalytic conversion of vanillin to creosol over bimetallic Ni2Fe@HZSM-5 using isopropyl alcohol (IPA) as a hydrogen donor proceeds via a tandem hydrogenation–deoxygenation pathway, facilitated by synergistic interactions between Ni and Fe metal sites. The proposed mechanistic scheme is based on experimental results, product distribution profiles, GC-MS analysis, and further quantitative analysis by GC-FID.

4.3.1 Stepwise Plausible Reaction Mechanism

Step 1: Hydrogenation of Vanillin to Vanillyl Alcohol

The initial step involves the reduction of the aldehyde group (–CHO) in vanillin to form vanillyl alcohol. This transformation is predominantly catalyzed by nickel (Ni) species, which are well known for their ability to activate and transfer hydrogen from IPA to electrophilic centers, such as carbonyl groups. The reaction likely follows the Meerwein–Ponndorf–Verley (MPV) type mechanism in which IPA acts as a hydrogen donor.

Step 2: Etherification to Di(isopropyl) Ether Derivative

Under the reaction conditions (acidic HZSM-5 support and excess IPA), vanillyl alcohol can undergo etherification with isopropyl alcohol to form 4-Hydroxy-3-methoxybenzyl alcohol, di(isopropyl) ether. This occurs via substitution of hydroxyl groups with isopropyl moieties. This intermediate is sometimes detected in GC-MS analysis, indicating a temporary protection or storage form of vanillyl alcohol under the reaction conditions. It is typically reversible and may be reconverted under catalytic action.

Step 3: Deoxygenation of Vanillyl Alcohol to Creosol

In the second step, vanillyl alcohol undergoes C–O bond cleavage, most likely via dehydroxylation, to yield creosol (4-methylguaiacol). This transformation is facilitated by

Fe sites, which are known to promote oxygen-removal processes through redox cycling and Lewis acidity.

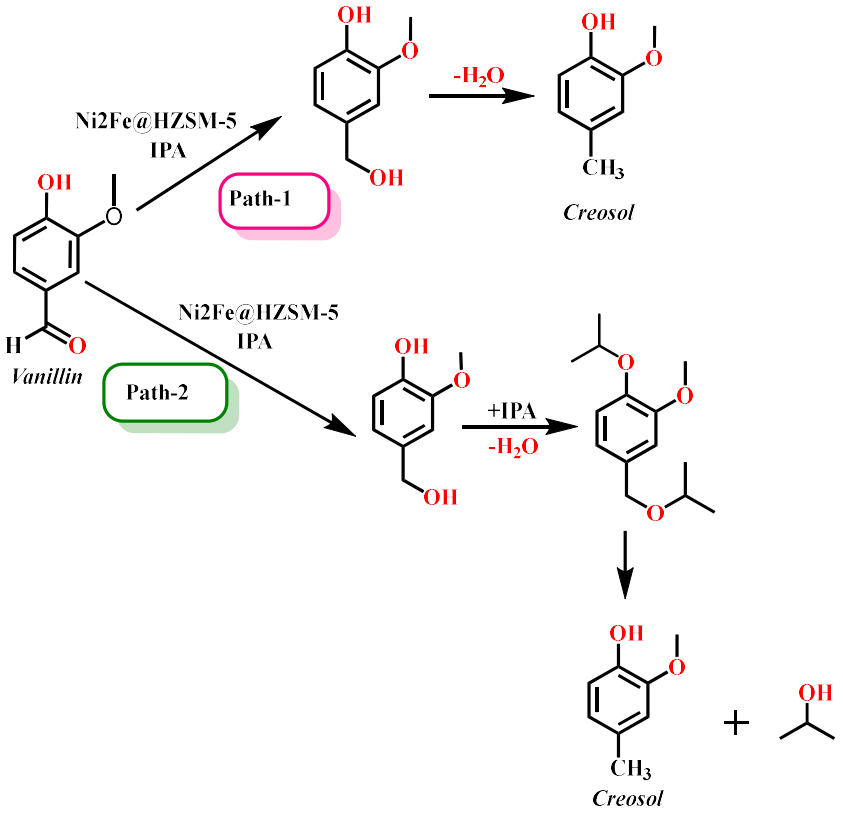

Figure 4.7: Catalytic Reaction Pathways

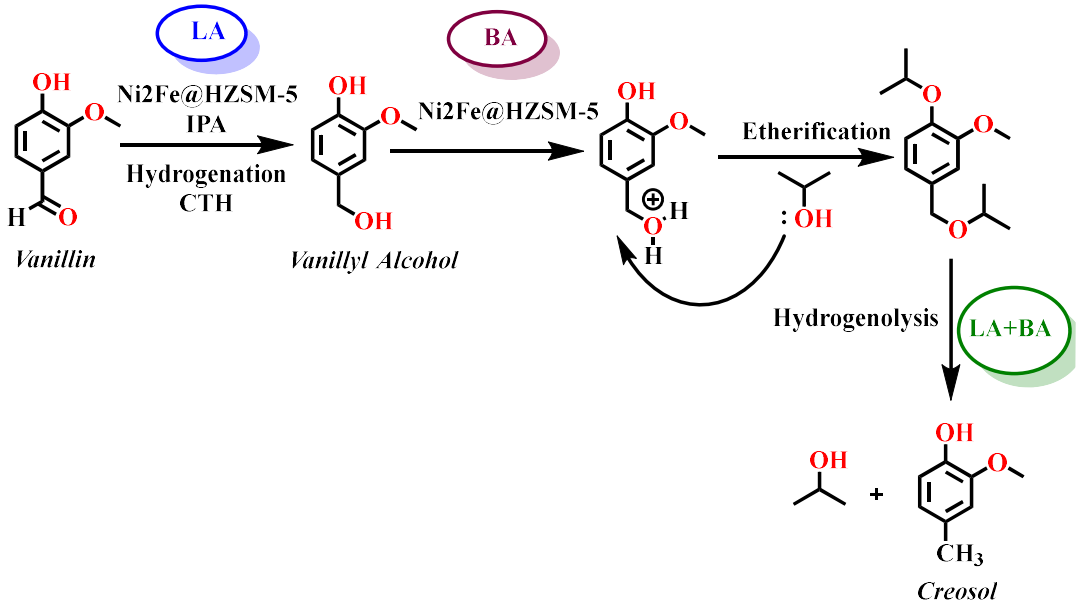

Figure 4.8: Plausible Catalytic Reaction Mechanism

4.3.2 Role and Fate of Di(isopropyl) Ether Intermediate

The formation of 4-Hydroxy-3-methoxybenzyl alcohol, di(isopropyl) ether is a transient step often observed under high IPA concentration and elevated temperatures. It represents an off-cycle intermediate formed via nucleophilic substitution between alcohol groups and IPA.

This compound can revert back to vanillyl alcohol under catalytic conditions, particularly in the presence of Fe or acidic sites that cleave the ether bond.

It does not accumulate significantly in the final reaction mixture, as confirmed by GC-MS, indicating its intermediate and reversible nature.

Its detection provides evidence of multiple active pathways and highlights the importance of reaction condition optimization (e.g., IPA amount, temperature, acidity).

4.3.3 Correlation with GC-MS Analysis

The GC-MS spectra show the presence of intermediates, including vanillyl alcohol and, occasionally, the di(isopropyl) ether, confirming the mechanistic hypothesis.

Quantification using a creosol calibration curve supports the kinetic pathway and confirms high yield and selectivity for the final product under optimized conditions.

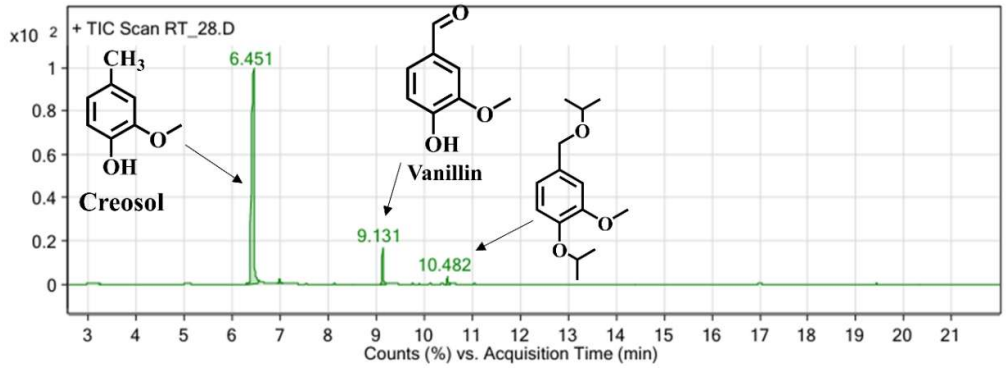

Integration Peak List

Peak	Start	RT	End	Height	Area	Area %
1	6.301	6.451	6.526	19204470.58	77214620.33	100
2	6.954	6.988	7.05	411182.56	807205.44	1.05
3	9.09	9.131	9.206	3198511.66	4876442.86	6.32
4	10.436	10.482	10.546	629958.82	1152083.49	1.49

Figure 4.10 GC-Chromatogram for optimized reaction condition: Vanillin (1mmol), IPA (25mL), Catalyst (Ni2Fe@HZSM-5, 30 wt.%), Temperature (200°C), Time (12h)

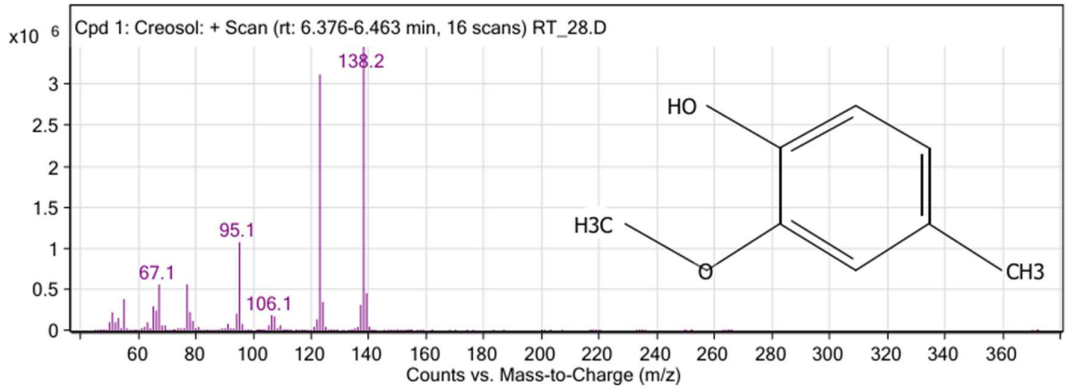

Peak List

m/z	Abund
55.1	371337.5
65.1	289449
67.1	559935
77.1	550063
95.1	1069232
123.1	3113332
124.1	344891.5
137.1	310910.5
138.2	3450544
139.1	453177.5

Figure 4.11: Mass spectrum of Creosol

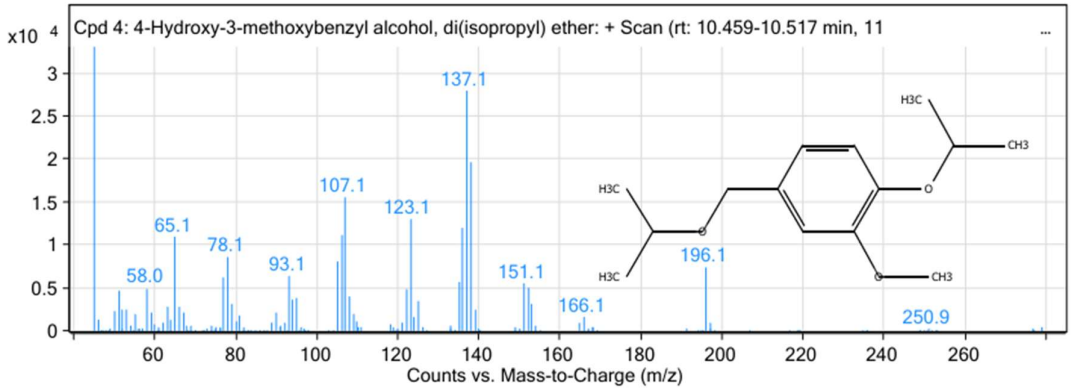

Peak List

m/z	Abund
45.1	32988.27
65.1	10938.91
78.1	8542.36
105	8004
106.1	11027.82
107.1	15483.91
123.1	12984.91
136.1	11963.18
137.1	27957.09
138.1	19530.82

Figure 4.12: Mass spectrum for ether

CHAPTER 5: CONCLUSION AND FUTURE SCOPE

5.1 Conclusion

In this research, the hydrodeoxygenation (HDO) of vanillin to creosol was successfully carried out using a bimetallic Fe–Ni_2 catalyst supported on H-ZSM-5. The study aimed to develop a cost-effective, efficient, and selective catalyst system for converting lignin-derived aromatic aldehydes into valuable alkylphenols. The catalyst was prepared via incipient wetness impregnation and subjected to thorough physicochemical characterisation to understand its structure–activity relationship.

5.2 Catalyst Characterisation

X-Ray Diffraction (XRD) analysis confirmed the integrity of the ZSM-5 framework post metal incorporation, with additional diffraction peaks indicating the presence of metal oxide phases.

BET Surface Area measurements revealed a decrease in surface area and pore volume after metal loading, consistent with successful dispersion of Fe and Ni particles within the zeolite matrix.

(SEM) images displayed uniformly distributed metal nanoparticles and retained pore morphology, contributing to accessible active sites..

FTIR and Pyridine-FTIR spectra confirmed the coexistence of Lewis and Brønsted acid sites, facilitating both dehydration and hydrogenation mechanisms during the transformation of vanillin to creosol.

5.3 Catalytic Evaluation

The Ni2Fe@ZSM-5 catalyst demonstrated excellent performance, achieving high vanillin conversion (84%) and notable selectivity towards creosol with 80% yield under mild reaction conditions. The reaction mechanism is presumed to proceed via metal-assisted hydrogenation followed by acid-catalyzed hydrogenolysis, supported by product analysis and literature precedents[54].

5.4 Quantitative Analysis

External calibration curves for both vanillin (reactant) and creosol (product) were established using standard solutions. The resulting linear regression equations exhibited high correlation coefficients of 0.99940 & 0.9943, respectively, validating their application

for accurate concentration determination. These data were used to calculate conversion rates, yields, and selectivity, forming the basis for assessing catalytic efficiency.

5.5 Future Scope

While the present study has laid a strong foundation for the valorization of lignin-derived aromatic compounds, there remain several promising directions for future exploration:

5.5.1 Catalyst Development

Further modification of metal composition, such as exploring different Fe/Ni ratios or incorporating promoters (e.g., Cu, Mo), may enhance selectivity and stability.

Utilization of hierarchical or mesoporous supports could improve diffusion properties and facilitate the transformation of bulkier lignin-derived substrates.

5.5.2 Process Optimization

Scaling up the reaction system using fixed-bed or continuous flow reactors could aid in evaluating the feasibility of industrial applications.

Kinetic and mechanistic studies should be pursued to elucidate reaction pathways and optimize operating parameters.

5.5.3 Feedstock Versatility

Testing the catalyst with real lignin depolymerization products or other relevant bio-oil components can assess robustness and practical applicability.

The influence of reaction medium components such as water, oxygenates, and inhibitors on catalyst activity should be systematically studied.

5.5.4 Sustainability and Integration

Catalyst recyclability and regeneration strategies need to be developed to enhance long-term usability.

Life cycle analysis and techno-economic evaluation will help in assessing the sustainability and commercial viability of the process within an integrated biorefinery setup.

References:

[1] P. McKendry, Energy production from biomass (part 1): overview of biomass, Bioresour Technol 83 (2002) 37–46. https://doi.org/10.1016/S0960-8524(01)00118-3.

[2] Y.X. Pang, N. Sharmin, T. Wu, C.H. Pang, An investigation on plant cell walls during biomass pyrolysis: A histochemical perspective on engineering applications, Appl Energy 343 (2023) 121055. https://doi.org/10.1016/j.apenergy.2023.121055.

[3] K.L. Patle, P. Pardhi, S. Pantawane, D.T. Sarve, Jayant. Ekhe, K.L. Wasewar, Nb_2O_5 supported metal-based heterogeneous catalysts for hydrodeoxygenation (HDO) of lignin-derived molecules: a powerful tool for generating fuel-additive products including hydrocarbons, Catalysis Reviews (2025) 1–53. https://doi.org/10.1080/01614940.2025.2453713.

[4] L.T. Mika, E. Cséfalvay, Á. Németh, Catalytic Conversion of Carbohydrates to Initial Platform Chemicals: Chemistry and Sustainability, Chem Rev 118 (2018) 505–613. https://doi.org/10.1021/acs.chemrev.7b00395.

[5] S.K. Singh, J.D. Ekhe, Solvent effect on HZSM-5 catalyzed solvolytic depolymerization of industrial waste lignin to phenols: superiority of the water–methanol system over methanol, RSC Adv. 4 (2014) 53220–53228. https://doi.org/10.1039/C4RA10240A.

[6] L.T. Mika, E. Cséfalvay, Á. Németh, Catalytic Conversion of Carbohydrates to Initial Platform Chemicals: Chemistry and Sustainability, Chem Rev 118 (2018) 505–613. https://doi.org/10.1021/acs.chemrev.7b00395.

[7] F. Wang, D. Ouyang, Z. Zhou, S.J. Page, D. Liu, X. Zhao, Lignocellulosic biomass as sustainable feedstock and materials for power generation and energy storage, Journal of Energy Chemistry 57 (2021) 247–280. https://doi.org/10.1016/j.jechem.2020.08.060.

[8] Y.X. Pang, N. Sharmin, T. Wu, C.H. Pang, An investigation on plant cell walls during biomass pyrolysis: A histochemical perspective on engineering applications, Appl Energy 343 (2023) 121055. https://doi.org/10.1016/j.apenergy.2023.121055.

[9] H. Zhang, S. Fu, X. Du, Y. Deng, Advances in Versatile Nanoscale Catalyst for the Reductive Catalytic Fractionation of Lignin, ChemSusChem 14 (2021) 2268–2294. https://doi.org/10.1002/cssc.202100067.

[10] D. Bourbiaux, J. Pu, F. Rataboul, L. Djakovitch, C. Geantet, D. Laurenti, Reductive or oxidative catalytic lignin depolymerization: An overview of recent advances, Catal Today 373 (2021) 24–37. https://doi.org/10.1016/j.cattod.2021.03.027.

[11] P. Mäki-Arvela, B. Holmbom, T. Salmi, D.Yu. Murzin, Recent Progress in Synthesis of Fine and Specialty Chemicals from Wood and Other Biomass by Heterogeneous Catalytic Processes, Catalysis Reviews 49 (2007) 197–340. https://doi.org/10.1080/01614940701313127.

[12] Y. Shao, Q. Xia, L. Dong, X. Liu, X. Han, S.F. Parker, Y. Cheng, L.L. Daemen, A.J. Ramirez-Cuesta, S. Yang, Y. Wang, Selective production of arenes via direct lignin

upgrading over a niobium-based catalyst, Nat Commun 8 (2017) 16104. https://doi.org/10.1038/ncomms16104.

[13] I.M.S. Anekwe, Y.M. Isa, B. Oboirien, Bioethanol as a potential eco-friendlier feedstock for catalytic production of fuels and petrochemicals, Journal of Chemical Technology & Biotechnology 98 (2023) 2077–2094. https://doi.org/10.1002/jctb.7399.

[14] A. Wittstock, M. Bäumer, Catalysis by Unsupported Skeletal Gold Catalysts, Acc Chem Res 47 (2014) 731–739. https://doi.org/10.1021/ar400202p.

[15] A. Corma, S. Iborra, A. Velty, Chemical Routes for the Transformation of Biomass into Chemicals, Chem Rev 107 (2007) 2411–2502. https://doi.org/10.1021/cr050989d.

[16] D.C. Elliott, Historical Developments in Hydroprocessing Bio-oils, Energy & Fuels 21 (2007) 1792–1815. https://doi.org/10.1021/ef070044u.

[17] X. Zhang, J. Tang, Q. Zhang, Q. Liu, Y. Li, L. Chen, C. Wang, L. Ma, Hydrodeoxygenation of lignin-derived phenolic compounds into aromatic hydrocarbons under low hydrogen pressure using molybdenum oxide as catalyst, Catal Today 319 (2019) 41–47. https://doi.org/10.1016/j.cattod.2018.03.068.

[18] S. Boullosa-Eiras, R. Lødeng, H. Bergem, M. Stöcker, L. Hannevold, E.A. Blekkan, Catalytic hydrodeoxygenation (HDO) of phenol over supported molybdenum carbide, nitride, phosphide and oxide catalysts, Catal Today 223 (2014) 44–53. https://doi.org/10.1016/j.cattod.2013.09.044.

[19] H.N. Pham, Y.J. Pagan-Torres, J.C. Serrano-Ruiz, D. Wang, J.A. Dumesic, A.K. Datye, Improved hydrothermal stability of niobia-supported Pd catalysts, Appl Catal A Gen 397 (2011) 153–162. https://doi.org/10.1016/j.apcata.2011.02.026.

[20] Y. Zheng, N. Zhao, J. Chen, Enhanced direct deoxygenation of anisole to benzene on SiO2-supported Ni-Ga alloy and intermetallic compound, Appl Catal B 250 (2019) 280–291. https://doi.org/10.1016/j.apcatb.2019.02.073.

[21] A. Kumar, A. Kumar, B. Biswas, J. Kumar, S.R. Yenumala, T. Bhaskar, Hydrodeoxygenation of m-Cresol over Ru based catalysts: Influence of catalyst support on m-Cresol conversion and methylcyclohexane selectivity, Renew Energy 151 (2020) 687–697. https://doi.org/10.1016/j.renene.2019.11.076.

[22] J.A. Hunns, M. Arroyo, A.F. Lee, J.M. Escola, D. Serrano, K. Wilson, Hierarchical mesoporous Pd/ZSM-5 for the selective catalytic hydrodeoxygenation of m-cresol to methylcyclohexane, Catal Sci Technol 6 (2016) 2560–2564. https://doi.org/10.1039/C5CY02072G.

[23] A. Kumar, A. Kumar, B. Biswas, J. Kumar, S.R. Yenumala, T. Bhaskar, Hydrodeoxygenation of m-Cresol over Ru based catalysts: Influence of catalyst support on m-Cresol conversion and methylcyclohexane selectivity, Renew Energy 151 (2020) 687–697. https://doi.org/10.1016/j.renene.2019.11.076.

[24] J. Chang, T. Danuthai, S. Dewiyanti, C. Wang, A. Borgna, Hydrodeoxygenation of Guaiacol over Carbon-Supported Metal Catalysts, ChemCatChem 5 (2013) 3041–3049. https://doi.org/10.1002/cctc.201300096.

[25] M. Kim, J.-M. Ha, K.-Y. Lee, J. Jae, Catalytic transfer hydrogenation/hydrogenolysis of guaiacol to cyclohexane over bimetallic RuRe/C catalysts, Catal Commun 86 (2016) 113–118. https://doi.org/10.1016/j.catcom.2016.08.022.

[26] F. Yang, D. Liu, Y. Zhao, H. Wang, J. Han, Q. Ge, X. Zhu, Size Dependence of Vapor Phase Hydrodeoxygenation of *m* -Cresol on Ni/SiO $_2$ Catalysts, ACS Catal 8 (2018) 1672–1682. https://doi.org/10.1021/acscatal.7b04097.

[27] C.M. Pichler, D. Gu, H. Joshi, F. Schüth, Influence of preparation method and doping of zirconium oxide onto the material characteristics and catalytic activity for the HDO reaction in nickel on zirconium oxide catalysts, J Catal 365 (2018) 367–375. https://doi.org/10.1016/j.jcat.2018.07.021.

[28] R. Shu, B. Lin, J. Zhang, C. Wang, Z. Yang, Y. Chen, Efficient catalytic hydrodeoxygenation of phenolic compounds and bio-oil over highly dispersed Ru/TiO2, Fuel Processing Technology 184 (2019) 12–18. https://doi.org/10.1016/j.fuproc.2018.11.004.

[29] J. Mao, J. Zhou, Z. Xia, Z. Wang, Z. Xu, W. Xu, P. Yan, K. Liu, X. Guo, Z.C. Zhang, Anatase TiO $_2$ Activated by Gold Nanoparticles for Selective Hydrodeoxygenation of Guaiacol to Phenolics, ACS Catal 7 (2017) 695–705. https://doi.org/10.1021/acscatal.6b02368.

[30] F. Yang, D. Liu, Y. Zhao, H. Wang, J. Han, Q. Ge, X. Zhu, Size Dependence of Vapor Phase Hydrodeoxygenation of *m* -Cresol on Ni/SiO $_2$ Catalysts, ACS Catal 8 (2018) 1672–1682. https://doi.org/10.1021/acscatal.7b04097.

[31] Y. Hong, H. Zhang, J. Sun, K.M. Ayman, A.J.R. Hensley, M. Gu, M.H. Engelhard, J.-S. McEwen, Y. Wang, Synergistic Catalysis between Pd and Fe in Gas Phase Hydrodeoxygenation of *m* -Cresol, ACS Catal 4 (2014) 3335–3345. https://doi.org/10.1021/cs500578g.

[32] C. Zhang, C. Jia, Y. Cao, Y. Yao, S. Xie, S. Zhang, H. Lin, Water-assisted selective hydrodeoxygenation of phenol to benzene over the Ru composite catalyst in the biphasic process, Green Chemistry 21 (2019) 1668–1679. https://doi.org/10.1039/C8GC04017F.

[33] X. Zhang, J. Tang, Q. Zhang, Q. Liu, Y. Li, L. Chen, C. Wang, L. Ma, Hydrodeoxygenation of lignin-derived phenolic compounds into aromatic hydrocarbons under low hydrogen pressure using molybdenum oxide as catalyst, Catal Today 319 (2019) 41–47. https://doi.org/10.1016/j.cattod.2018.03.068.

[34] T.M. Sankaranarayanan, A. Berenguer, C. Ochoa-Hernández, I. Moreno, P. Jana, J.M. Coronado, D.P. Serrano, P. Pizarro, Hydrodeoxygenation of anisole as bio-oil model compound over supported Ni and Co catalysts: Effect of metal and support properties, Catal Today 243 (2015) 163–172. https://doi.org/10.1016/j.cattod.2014.09.004.

[35] R. Brayner, F. Bozon-Verduraz, Niobium pentoxide prepared by soft chemical routes: morphology, structure, defects and quantum size effect, Physical Chemistry Chemical Physics 5 (2003) 1457–1466. https://doi.org/10.1039/b210055j.

[36] J.M. Jehng, I.E. Wachs, Structural chemistry and Raman spectra of niobium oxides, Chemistry of Materials 3 (1991) 100–107. https://doi.org/10.1021/cm00013a025.

[37] J. Zhang, J. Gu, R. Shan, H. Yuan, Y. Chen, Advances in thermochemical valorization of biomass towards carbon neutrality, Resour Conserv Recycl 212 (2025) 107905. https://doi.org/10.1016/j.resconrec.2024.107905.

[38] M. Fache, B. Boutevin, S. Caillol, Vanillin Production from Lignin and Its Use as a Renewable Chemical, ACS Sustain Chem Eng 4 (2016) 35–46. https://doi.org/10.1021/acssuschemeng.5b01344.

[39] J. Eun, J. Kim, H.B. Kim, D.H. Kim, J.-W. Choi, K.H. Kim, C.-J. Yoo, S. Jin, K. Kim, H. Lee, C.S. Kim, K.-Y. Lee, J.S. Yoo, S.-J. Han, K. Jeong, J.-M. Ha, Production of high-carbon-number hydrocarbon bio-aviation fuels *via* catalytic hydrogenation of vanillin and non-catalytic condensation: a mechanistic study with DFT and experimental insights, Green Chemistry (2025). https://doi.org/10.1039/D5GC00281H.

[40] X. Wang, Z. Zhang, Z. Yan, Q. Li, Y. Zhang, Catalysts with metal-acid dual sites for selective hydrodeoxygenation of lignin derivatives: Progress in regulation strategies and applications, Appl Catal A Gen 662 (2023) 119266. https://doi.org/10.1016/j.apcata.2023.119266.

[41] W. Jin, L. Pastor-Pérez, D. Shen, A. Sepúlveda-Escribano, S. Gu, T. Ramirez Reina, Catalytic Upgrading of Biomass Model Compounds: Novel Approaches and Lessons Learnt from Traditional Hydrodeoxygenation – a Review, ChemCatChem 11 (2019) 924–960. https://doi.org/10.1002/cctc.201801722.

[42] W. Lei, Y. Fu, S. Gu, S. Qiu, J. Chang, Synergistic Cu-Pd Nanocatalysts on MOF-Derived N-Doped Carbon for Selective Hydrogenolysis of Lignin to Aromatic Monomers, Catalysts 15 (2025) 455. https://doi.org/10.3390/catal15050455.

[43] D. Luo, X. Gao, P. Lu, J. Hu, Catalytic Transfer Hydrodeoxygenation of Lignin-Derived Phenolic Compounds over RuMo/NC with Isopropanol as *In Situ* Hydrogen Source, Energy & Fuels 39 (2025) 8120–8128. https://doi.org/10.1021/acs.energyfuels.5c00475.

[44] J. Zhang, X. Kuang, L. Zhu, X. Xiao, Z. Zhou, F. Qi, Sustainable production of cyclohexanones through hydrodeoxygenation of lignin-derived phenolics over PdFe/HZSM-5 catalysts, Fuel 383 (2025) 133863. https://doi.org/10.1016/j.fuel.2024.133863.

[45] S. Deepika, A. Pandurangan, K. Parthiban, R. Tschentscher, Exploring the efficacy of Re-Ni embedded KIT-6/H-Mor catalysts for renewable energy – A comprehensive experimental and theoretical (DFT) exploration, Bioresour Technol 415 (2025) 131698. https://doi.org/10.1016/j.biortech.2024.131698.

[46] X. Yu, Q. Chen, Z. Hu, Q. Zhu, X. Kong, Selective Hydrogenation of Lignin-Derived Phenols by Ultrafine Co–Ni Bimetallic Alloy Embedded on Dendritic Mesoporous Silica Nanoreactor, ACS Sustain Chem Eng 13 (2025) 2853–2863. https://doi.org/10.1021/acssuschemeng.4c09150.

[47] Q. Han, M.U. Rehman, J. Wang, A. Rykov, O.Y. Gutiérrez, Y. Zhao, S. Wang, X. Ma, J.A. Lercher, The synergistic effect between Ni sites and Ni-Fe alloy sites on hydrodeoxygenation of lignin-derived phenols, Appl Catal B 253 (2019) 348–358. https://doi.org/10.1016/j.apcatb.2019.04.065.

[48] S.K. Singh, K. Nandeshwar, J.D. Ekhe, Thermochemical lignin depolymerization and conversion to aromatics in subcritical methanol: effects of catalytic conditions, New Journal of Chemistry 40 (2016) 3677–3685. https://doi.org/10.1039/C5NJ02916C.

[49] S.K. Singh, J.D. Ekhe, Cu–Mo doped zeolite ZSM-5 catalyzed conversion of lignin to alkyl phenols with high selectivity, Catal Sci Technol 5 (2015) 2117–2124. https://doi.org/10.1039/C4CY01700E.

[50] S.K. Singh, J.D. Ekhe, Cu–Mo doped zeolite ZSM-5 catalyzed conversion of lignin to alkyl phenols with high selectivity, Catal Sci Technol 5 (2015) 2117–2124. https://doi.org/10.1039/C4CY01700E.

[51] H.T. Kreissl, M.M.J. Li, Y.-K. Peng, K. Nakagawa, T.J.N. Hooper, J. V. Hanna, A. Shepherd, T.-S. Wu, Y.-L. Soo, S.C.E. Tsang, Structural Studies of Bulk to Nanosize Niobium Oxides with Correlation to Their Acidity, J Am Chem Soc 139 (2017) 12670–12680. https://doi.org/10.1021/jacs.7b06856.

[52] E.W.V.R.D.S. H.L.D. Rollmann, Characterization of Solid Materials and Heterogeneous Catalysts, Wiley, 2012. https://doi.org/10.1002/9783527645329.

[53] D.T. Sarve, S.K. Singh, J.D. Ekhe, Ethanol dehydration to diethyl ether over ZSM-5 and β-Zeolite supported Ni W catalyst, Inorg Chem Commun 139 (2022) 109397. https://doi.org/10.1016/j.inoche.2022.109397.

[54] H. Zhang, T. Yang, Y. Tong, B. Li, J. Wang, R. Li, FeNi/hexagonal boron nitride for catalytic hydrodeoxygenation of guaiacol derived from lignin to cycloalkanes, Fuel 368 (2024) 131620. https://doi.org/10.1016/j.fuel.2024.131620.